From Concept to the Prototype of Heart Turcica Centrifugal: Development and in Vitro Tests of the First Implantable Centrifugal Left Ventricular Assist System in Turkey

by

Gökhan Yıldız

A Thesis Submitted to the
Graduate School of Engineering
in Partial Fulfillment of the Requirements for
the Degree of

Master of Science
in
Mechanical Engineering

Koc University

July 2008

Koc University

Graduate School of Sciences and Engineering

This is to certify that I have examined this copy of a master's thesis by

Gökhan Yıldız

and have found that it is complete and satisfactory in all respects,
and that any and all revisions required by the final
examining committee have been made.

Committee Members:

_____

Assoc. Prof. Dr. Ismail Lazoglu (Advisor)

_____

Assoc. Prof. Dr. Metin Muradoglu

_____

Asst. Prof. Dr. Erdem Alaca

_____

Asst. Prof. Dr. Mehmet Sayar

_____

Asst. Prof. Dr. A. Fethi Okyar

Date: _____

ABSTRACT

A prototype of a new implantable centrifugal heart pump was developed as a Left Ventricular Assist Device (LVAD) for the treatments of end-stage cardiac failures. In the development of Heart Turcica Centrifugal (HTC), Computational Fluid Dynamics (CFD), Computer Aided Design / Engineering / Manufacturing (CAD/CAE/CAM) tools were utilized in various stages from conceptual design to the final prototype. In this research, flow and performance characteristics of various centrifugal blood pumps were analyzed in details. A prototype of HTC was manufactured with high precision by the high speed production techniques in Computer Numerical Control (CNC) machines. In this thesis, the development stages of the HTC are introduced and the results of the in vitro tests of the HTC are presented.

ÖZET

Sol Karıncık Destek Aygıtı (SKDA) kalp hastalıklarının tedavisinde kullanılmak üzere yeni bir vücut içine yerleştirilebilir sentrifugal pompanın prototipi geliştirildi. Bu Sentrifugal Türk Kalbi'nin (STK) geliştirilmesinde Hesaplamalı Akışkanlar Dinamiği (HAD), Bilgisayar Destekli Tasarım / Mühendislik / Üretim (BDT / BDM / BDÜ) araçları, genel kavram tasarımından son prototip üretimine kadar kullanılmıştır. Bu çalışmada, birçok sentrifugal kalp pompasının akışkan ve performans karakteristikleri incelendi. Bu STK'nın prototipleri Bilgisayar destekli Numerik Kontrollü makinelerde yüksek hassasiyetle üretilmiştir. Bu tezde, STK'nın gelişim süreci ve vücut dışı deneylerinin sonuçları sunulmuştur.

ACKNOWLEDGEMENTS

I would like to acknowledge to my friends Murat Ötkür for his guidance and great support in using the Computer Numerically Controlled (CNC) machine, Mustafa Kaymakçı in helping the development of the G-codes and toolpaths, Onur Demir being the great partner in the project, Aydın Varol and Durul Ulutan for their patience.

I would like also to acknowledge to my advisor Ismail Lazoglu for his unique support and patience in completion of this thesis.

This thesis is dedicated to my parents Şerife Yıldız and Ahmet Yıldız, and my brothers Okan Oktay Yıldız and Kadir Atacan Yıldız.

TABLE OF CONTENTS

LIST OF TABLES

LIST OF FIGURES

NOMENCLATURE

r_1 *and* r_2	Radius of runner at inlet and outlet
v	Absolute velocities
g	Acceleration due to gravity
β_1 *and* β_2	Runner vane angles
u	Peripheral velocities
w	Relative velocities
ω	Angular velocity
V_a	Axial component of the velocity vector
V_m	Radial component of the velocity vector
V_u	Tangential component of the velocity vector
τ	Net torque of the rotor
M	Mass of the fluid
t	Time
E_o	Rate of energy transfer
U	Linear velocity of the rotor at radius r
H	The energy transferred per unit mass
c *and* c_a	Chord and the axial chord
h	The blade height or span
s	The pitch or spacing
γ	The stagger angle
ΔP	Pressure difference

Chapter 1

INTRODUCTION

Over the last decade, rapid advances have occurred in the development of artificial hearts and heart assist devices. These have been fueled by the continuous concern over the prevalence of cardiovascular disease and associated deaths and by the inability of a generation of fixed volume blood pumps to adequately serve for long-term cardiac assistance. Although there are several types of heart assist devices such as axial, pulsatile, centrifugal etc., this study focuses only on the development of a reliable and permanently implantable centrifugal blood pump as a left ventricular assist device.

The focus of much cardiovascular research in recent years has been to develop devices that can assist or replace the heart in its function as a blood pump. The two primary categories of devices are Total Artificial Hearts (TAH's) and Ventricular Assist Devices (VAD's). With this study a reliable and implantable centrifugal blood pump is designed in several steps by developing and refining.

Centrifugal pumps have many uses such as turbochargers in automobiles, large industrial pumps and hydraulic pumps. These pumps have been used for over a century in various applications and have a huge source of performance data on which to base new designs.

However, the use of centrifugal pumps as blood pumps has a rather short history. The performance data for centrifugal blood pumps is limited in the literature. Often, the available performance data for a given design is tested using water as the test fluid, rather

than blood like fluids. This leads to hydraulic performance data that does equate to actual in vivo performance. Another dilemma of centrifugal blood pumps is the design approach, which is to take a best guess at a good design and then refine the design through trial and error. The disadvantage of a trial and error approach is the amount of time and cost involved. In order to expedite the design process, it was determined that a table of performance data involving centrifugal pumps of small scale and realistic fluid viscosity would be invaluable. Computational Fluid Dynamics(CFD) methods play very important roles in prediction of the performance of the several impeller designs. The production method follows these steps: 1) Computer Aided Design (CAD) of the impeller with design softwares, 2) Computer Aided Manufacturing (CAM) that is development of the production codes with computers, 3) Production the parts of the pump with Computer Numerically Controlled (CNC) Machines.

The goal of this research is to develop a reliable and permanently implantable centrifugal blood pump as a left ventricular assist device. In order to achieve this goal first concentrated on which geometric factors of an impeller are the most significant that affect the performance and secondly several designs were developed by changing these variables.

Chapter 2 provides necessary background and literature review on TAH's and VAD development. The fundamentals of TAH's and VAD development, physics of blood pumps and previous designs as TAH's and VAD are reviewed.

Chapter 3 describes the specifications that a blood pump should have and general theory of the centrifugal pump design is presented. Thereafter the design process of the developed centrifugal blood pump is explained, including the development the impeller and the housing.

Computational Fluid Dynamics approach is explained in Chapter 4, where the methodology that is employed to predict the performance of the different types of designs

is described. In addition to that, several methodologies are explained and compared for more accurate prediction of the performance data.

In chapter 5, different designs developed through the study are described. The tests that applied to them are presented and the theoretical results added to them together with the discussion of these results.

The thesis is concluded with a short summary of the performed study and future research work.

Chapter 2

LITERATURE REVIEW

Continuous flow blood pumps were developed very early by DeBakey, Gibbons, and Kantrowitz, who are also the developer of the heart-lung machines used for cardiopulmonary bypass. Dr. Wesolowski published on the role of the pulse in the maintenance of normal physiology in the systemic circulation during heart-lung bypass in 1955 [9]. It is shown by these early experiments that pulsatile flow was not critical to the maintenance of the integrity of either the pulmonary or systemic circulation. The continuous flow blood pumps were described first in the article named "An ideal heart pump with hydrodynamic characteristics analogous to the mammalian heart", by Saxton and Andrews in 1960 [10]. They claimed that the centrifugal blood pump may have several advantages over the positive displacement pulsatile devices. In their article they stated that it was smaller in size, required much less power with a minimum of moving parts, and required no valves or flexing plastic chambers. In addition, they observed that the flows were sensitive to inflow and outflow pressures, suggesting some level of autocontrol. This behavior is also mentioned by Egemen Tüzün from Texas Heart Institute in 15 June 2007 in Turkish Society for Artificial Organs and Support Systems (TUYOD)'s first Artificial Organs Conference. He also suggested that this behavior makes centrifugal blood pumps most suitable devices for total artificial hearts.

On the other hand, there are two primary disadvantages of centrifugal blood pumps. One is the unknown shear stresses within the pumping chamber that can result in blood cell

damage. The second disadvantage is that continuous flow requires higher output volumes than pulsatile flow in animals. Excessive blood cell injury caused by high shear stress can result in hemolysis. This has lead to several questions for many years. Two of these questions are; “How much plasma-free hemoglobin is too much?” and “What is the toxicity of a high plasma-free hemoglobin within the organism?”. Therefore, the effects of various levels of intravascular hemoglobin were examined by several researchers. Earlier than these heart pump studies, Ottenberg [26] reported that the renal threshold in man for hemoglobin was above 150 mg. This means that when the plasma-free hemoglobin exceeds 150 mg, it is excreted into the urine. His studies also demonstrated that up to 8g of hemoglobin was cleared in 20 h. In 1949, Maluf [27] reported that in patients with dehydration or shock, the consequences of high plasma-free hemoglobin could cause renal failure at otherwise benign levels. Latham[28] reported that plasma-free hemoglobin at levels up to 150 mg was conjugated in the liver to haptoglobin, which was cleared through the reticuloendothelial system.

Common problems possible with blood pumps are hemolysis and/or thrombus formation. High shear stress and a tortuous flow path are two conditions that can cause hemolysis. Thrombus formation is a complex function of physiological conditions, biocompatibility of blood contacting surface, and the fluid dynamic characteristics of blood flow within a flow domain. Generally, thrombus formation occurs in regions of high shear stress, turbulence and/or poor blood biocompatibility followed by exposure to regions of re-circulation (i.e. vortices) and/or stagnation. Rafferty et al. [11] in 1968 developed a centrifugal blood pump which supplied a continuous flow. This pump based on a principle that they called as “forced vortex principle”. This pump became known as the “Biopump” because it had extremely low hemolysis rates and it was commercialized in 1976. Dorman and colleagues in 1969 [12] reported on the development of the velocity head pump with an

index of hemolysis less than 0.01 and efficiency of 17 to 37 % and presented the results in animals being perfused for 1 – 3 h.

Bernstein et al. [13] in 1974 published the results of a series of experiments described as a nonthoracotomy prolonged ventricular bypass after successfully running a continuous flow pump in the calf for 24 h. 21 % mg was the limit for the plasma-free hemoglobin. However, there was a decrease in platelets and there was normal clotting of the blood, with only minor renal emboli. With the Biomedicus-type pump, seal failure was often associated with an increase of plasma-free hemoglobin in excess of 300 mg%.

Golding et al. [14] in 1979 reported some initial clinical experiences with the Medtronic pump and reported good hemodynamic support of the patients with plasma-free hemoglobins of 39 mg% at 24 h. After that, the plasma-free hemoglobins dropped to 25.5 mg% for the remaining perfusion time.

Golding et al. [15] in 1980 started a series of calf experiments in which a centrifugal pump was attached to both the right and left ventricles, which were subsequently fibrillated, and these early experiments had calves surviving up to 34 days on a totally nonpulsatile perfusion. Reports in the literature of the successful use of centrifugal pumps encouraged investigators to develop a variety of continuous-flow blood pumps. A series of articles published from 1981 through 1985 by Bramm and Olsen et al. [16,17,18] described a magnetically suspended impeller blood pump where there were no contact bearings on the free-floating impeller.

Wampler et al. [19] in 1988 described a miniaturized axial pump mounted on the tip of the catheter that could be passed from the femoral artery into the left ventricular chamber as an assist device. The rotational speed of the impeller of this pump was between 25.000 and 35.000 rpm, and the flow rate was the 3.5 L/min. However the damage to the red blood cells was very low. Dr. Wampler stated that if this pump were to produce 10 g of free

hemoglobin per day at 3 L/min of flow, it would have to lyse one blood cell for every 56.000 red blood cells that passed through the pump.

Monties and Mesana developed a rotary blood pump which was based on the Wankle engine principle [20].

Akamatsu et al. [21] in 1990 developed a magnetically suspended impeller pump which was acquired by the Terumo Corporation. This pump could maintain a sheep alive in excess of 2 years. The Houston group, with Dr. Nose as the leader, developed the Baylor Gyro pump, which underwent a series of modifications and is presently commercially available for use as a cardiopulmonary bypass pump [22].

Doctors DeBakey and Noon worked with a group of engineers from NASA to develop a very small axial pump to be used as a left ventricular assist device. This pump has strong magnets set in the tips of the inducer impeller vanes that minimize the air gap between the rotor and the stator of the driving brushless-DC motor. In 2000, the pump was implanted in 25 patients in Europe and has undergone extensive testing and evaluation on the bench as well as in animals in preparation for an application to the Food and Drug Administration (FDA) for approval for clinical use as a bridge to transplant within the United States [23]. The bearings of this pump have proven extremely reliable in bench tests exceeding 2 years. The Nimbus Corporation also developed a miniaturized axial flow pump similar in size and configuration to the DeBakey VAD [24]. Nimbus in cooperation with ThermoCardio Systems, Inc. developed another device known as the HeartMate II. A third and similar axial flow pump was developed by Jarvik and is referred to as the Jarvik 2000 [25].

In 2000, a magnetically suspended centrifugal pump is developed in the Utah Artificial Heart Institute, in combination with MedQuest Products, Inc. and the University of Virginia. This pump has been ex vivo tested in one animal study. Dr. Antaki and the Pittsburgh group developed the Streamliner axial flow pump with the impeller suspended in magnetic bearings.

The 1960 publication by Saxton and Andrews [10] pointed out that the flow through the centrifugal pump was sensitive to inflow and outflow pressures, suggesting some level of autocontrol. At that point, the physiological controller for rotary blood pumps had not been well developed. The goal of that controller would be to automatically make quick changes in the pump's performance in response to one or more precisely monitored, derived, or determined cardiovascular parameters.

The only mechanism to control the continuous flow of rotary blood pumps is to increase or decrease the speed of rotation. These modifications in speed must be keyed to some physiological parameter. With the unavailability of highly reliable external sensors, engineers have developed algorithms utilizing the available parameters such as motor rpm and motor current. There is a plenty of work done in this arena, but there is much more to be done because these pumps are to be implanted in patients as a permanent left ventricular or right ventricular assist device. The DeBakey ventricular assist device has been used in patients in Europe utilizing a flow probe on the outflow tract as an indicator to the attendees to increase or decrease pump rpm. This has worked very satisfactorily as a temporary bridge to cardiac transplantation, but a closed loop automatic system would be far more desirable in the permanent application of these devices.

A large variety of blood pumps designed to be used as total artificial hearts or cardiac replacement devices, as well as a variety of ventricular assist devices, are presently either on the market or are being developed and soon will be on the marketplace.

Positive displacement or pulsatile pumps are first generation pumps. Examples of these first generation pumps are the CardioWest total artificial heart, the Thoratec biventricular assist devices, the TCI HeartMate I VAD, the Novacor VAD, the HeartSaver by Worldheart, and the Pierce Lion Heart.

The rotary blood pumps with contact bearings and/or seals can be classified as the second generation pumps. These second generation pumps would have contact bearings,

either within the bloodstream or protected from the bloodstream by seals. Examples of this group of blood pumps would include the MicroMed DeBakey VAD, the Jarvik 2000 VAD, and the Nimbus-TCI HeartMate II VAD.

The rotary blood pumps with only magnetic bearings can be classified as the third generation pumps. On the other hand, rotary blood pumps without mechanical or touching bearings can be also treated as the third generation pumps. These pumps contain magnetic bearings and hydrodynamic bearings. Examples would include the Terumo VAD, the MedQuest Heartquest VAD, the University of Pittsburgh Streamliner VAD, and the centrifugal pump being developed at the Cleveland Clinic by Dr. Leonard Golding, the VentraAssist, hydrodynamically suspended centrifugal pump by Dr. Woodward and associates, and the Cora Heart by Dr. Monties.

These systems mentioned here are expensive for Turkish patients having heart failures, however the solution for the Turkish patients is implementing an artificial heart into the body, because there are 500 000 patient having heart failure and every year 2 to 3000 of them need heart transplantation [29]. However, only 20 heart transplantations can be held each year, because finding donors is difficult. Therefore development of an artificial heart assisting system in Turkey has been the motivation in this study.

Chapter 3

CENTRIFUGAL BLOOD PUMP DESIGN

3.1 Introduction

Development of an antitraumatic antithrombogenic and durable blood pump is a very difficult task. There are many design criteria to satisfy of a clinically effective and safe cardiac prosthesis. The design includes optimal size, satisfactory endurance characteristics, and efficient operation, antitraumatic features for the blood, and antithrombogenicity and biocompatibility. Unfortunately, these design criteria are very often opposing features. For example, size versus endurance, efficiency versus thrombogenicity, and antitraumatic features versus antithrombogenic features are particular opposing characteristics. The dilemma in properly designing a cardiac prosthesis is how to optimize the opposing design parameters, the opposing material characteristics and the opposing design requirements. Thus, designing a good cardiac prosthesis has been very difficult. As Nose [1] stated that the development of a good, clinically effective, and safe cardiac prosthesis was only possible through the efforts of an experienced cardiac prosthesis designer. However, for this development engineers and surgeons from several areas work together.

3.2 Classification

Considering all the blood pumps needed for various clinical situations, pumps are generally classified into 3 categories. The most commonly used blood pumps are for

cardiopulmonary bypass. If the pump performs safely and effectively for 2 days, it is generally satisfactory as a cardiopulmonary bypass pump even though its typical clinical usage is often less than 6h. To develop a blood pump for 2 days is a rather easy task because this pump is used as an extracorporeal cardiopulmonary bypass pump. During cardiopulmonary bypass procedures, subjects are fully heparinized, and it is unnecessary to consider the antithrombogenetic features of the pump. Additionally, the typical usage for this pump is less than 6h, and device endurance characteristics need not be considered. Development of a 2 day antitraumatic blood pump is relatively easy task, so that it is inexpensive and therefore accessible to the 800,000 patients who annually require such a device. In the event of transient cardiopulmonary failure, the blood pump would typically be required to operate safely and effectively for 2 weeks. This period is the most sensitive and active immunological periods of time. During the first 2 week postoperative period, the blood clotting tendencies are quite active and typically produce white thrombus even though the blood coagulation time of the subject has traditionally been extended to approximately 2 times the normal level through the administration of drugs.

The second category of blood pumps satisfies other clinical needs such as circulatory support for postcardiotomy cardiac failures, extracorporeal membrane oxygenation (ECMO), and percutaneous cardiopulmonary support (PCPS). These particular blood pumps should meet a minimum 1 month failsafe operation.

The third category of clinically needed pumps is applied to long-term ventricular assistance for bridge to transplantation or for bridge to recovery. These pumps should typically last longer than 6 months and up to 2 years. In the past, pumps used for bridge to transplantation satisfactorily achieved their objectives if they were durable for up to 6 months. However, now with the longer waiting periods for patients to obtain donor hearts,

it is essential that a pump operates for at least 1 year or longer. Also, long-term circulatory assistance has been further extended with the current discovery of myocardial recoveries after prolonged assistance. Now to effectively sustain the patient, the device lifetime should be at least 2 years. Thus, the design objectives of the third category implantable device should be intracorporeal durability for longer than 2 years. Thus, the mechanical and electrical components of the device should endure for at least 5 years. To expect an operational implantable electrical system, it is essential that an implantable package be hermetically sealed to avoid any fluid invasion. In addition, it is also essential to maintain the lowest temperature possible inside the implantable electrical component package. The clinical needs for the pumps from this third category are quite substantial. According to the projection made by the National Heart, Lung, and Blood Institute (NIHLB), at least 60,000 patients annually require such devices in the USA alone. Because the number of available donor hearts is limited and only in the range of $1/20^{th}$ the number required by patients, the development of an effective, durable, and reliable, yet small, permanently implantable cardiac prosthesis is mandatory.

3.3 Antithrombogenic Effects and Bioadaptability of Cardiac Prostheses

Blood reacts to contact with any foreign material and depending on that foreign surface, red thrombus may form immediately. In general, after a cardiac prosthesis implantation, various types of surgical insults also affect a patient's blood coagulation process. Therefore, according to Nose[1] red thrombus generally tends to form after implantation of a cardiac prosthesis during the first 2 days if the device is not properly designed. This is also a similar physiological response occurring after organ transplantation, known as super acute rejection. A 2 day period is also required for a recipient's bioadaptation to the implanted cardiac prosthesis. During this period, careful regulation of the implanted device

is necessary. However, it generally becomes easier to control the operation of an implanted device after this 2 day period.

During the initial 2 weeks after implantation, the recipient's physiological systems are fighting this implanted foreign device and its mode of operation. During this time period, circulatory abnormalities are generally observed. They include higher peripheral resistance, higher venous pressure, and higher circulating blood volume. This 2 week period is also the immunological system's most active stage, and acute rejection of the implanted device tends to occur because of the immunologically active state of the recipient. White thrombus has a tendency to form inside the implanted prosthesis during this period of time.

Fortunately, after 2 weeks of implantation, white thrombus is more likely not to form inside a rotary blood pump. All the blood contacting surfaces of the rotary blood pump are pacified by coating them with the proper protein that results in the surface of the device being quite antithrombogenic, usually for a long period of time. The chance of a thromboembolic incident may not occur even after 6 months or more; however, the third reaction eventually occurs after implantation, but it is not induced by the implanted device itself. Generally, it is caused by a hyperplastic reaction of the device host interface. This situation is somewhat different when a pulsatile blood pump is implanted. A pulsatile blood pump requires a pumping chamber, which is composed of an elastic and compressive material. Because of its repeated flex motion, the surface of the pumping chamber is not always the same. Very often elongation or microcracks of the pumping chamber surface reveal a new blood contacting surface. Thus, this basic phenomenon is only applicable to a nonpulsatile rotary blood pump. The rotary blood pump is basically constructed of components that are structurally solid and nondeformable. After the biocompatible native protein deposition on the surface takes place in 2 weeks, this surface remains unchanged for a long time period. Unfortunately, this is not applicable for the mating surface of the bearings in a rotary blood pump.

3.4 Development of an Antitraumatic Blood Pump

Generally, if the pump is hydraulically efficient, it is an antitraumatic blood pump. Avoiding backflow, high shear stress regions, and high temperature regions inside the blood chamber are essential in designing a good antitraumatic pump. The blood contacting surface roughness also affects the hemolysis rates. In general, the blood trauma introduced by a rotary blood pump is incrementally increased when the pressure head is increased. Thus, the normalized index of hemolysis (NIH) should be studied in at least 3 different pressure head conditions, namely, 100 mmHg (LVAD condition), 350 mmHg (Cardiopulmonary bypass (CPB) condition),and 500mmHg (Percutaneous cardiopulmonary support(PCPS) System). The pump with antitraumatic features acceptable for cardiopulmonary bypass should be able to demonstrate several times lower hemolysis rates when used for left ventricular assistance.

Any pump exhibiting an NIH level less than 0.02g/100 L at 500 mmHg and less than 0.004 g/100 L at 100 mmHg is considered to be acceptable. Antitraumatic properties of erythrocytes are stronger than those of platelets and leukocytes. Therefore, more traumas to platelets and leukocytes may occur when the hemolysis rates are increased. Even though it is necessary to investigate these traumatic effects, the NIHs are generally considered an acceptable indicator of blood trauma induced by a pump. To qualify for a clinically acceptable 2 day pump, 6 h cardiopulmonary bypass studies and 2 day paracorporeal left heart bypass implantation studies should be satisfactorily performed.

A design objective for the 3rd category pump is to make it durable, not only mechanically but also electrically, inside the body environment. Mechanical endurance characteristics of a rotary blood pump are dictated by the integrity of its moving parts, namely, the impeller. Also, the operational life of the impeller is dictated by the integrity of

its bearing system so the selection of a durable bearing system is the key in designing a durable rotary blood pump. Wear resistant bearings should be developed to achieve a permanent rotary blood pump. The wear of the bearings is imposed by the rotation of the male bearings inside the female bearings. Thus, a basic principle for a rotary blood pump is that its endurance characteristics improve when the impeller speed is lowered and the required torque for the impeller rotation is lowered. The size of the device would be smaller when the speed of the impeller is increased. However, to anticipate durable designs for the pump, over miniaturization should be avoided unless limited operational life is required. Design optimization of the overall size of the device should be seriously considered based upon the necessary clinical duration for such a device.

The mechanical endurance characteristics of the bearings should be proven for at least 2 years of life and possibly for 5 years in the case of a permanently implantable device. All plastic components should be replaced with durable and biocompatible metallic components. The primary choice of metallic components is generally the titanium alloys. The entire pump-actuator package should be hermetically sealed to prevent body fluid invasion. Electrical cables should be mechanically anti-flux structures having materials with anti-moisture coatings and coverage. To avoid any added electrical failures imposed by higher temperatures inside the electronics package, the highest temperature inside the package should be less than 10°C higher than the body temperature.

The temperature for tissue and blood contacting surface should be less than 43°C. To provide this environment, it is necessary to consider sufficient heat sink structures. The entire intracorporeal package should have the proper size, shape, and surface structures, providing an anatomically and tissue compatible device. Antipanus formation intraventricular cannulas with air and blood leakage free attachment structures should be provided. The inflow conduit to the pump should have a structurally non-deforming design withstanding the negative pressures. In addition, its basic structure should be water and gas

impermeable. Initially, the design of the permanently implantable pump system could be a vented system and the intracorporeal subsystem only the pump actuator package. The miniaturized wearable controller and power packages could be outside of the body. However, the final system should be a totally implantable system with an implantable power controller module. Routine power supply by wearable power packages should be made through the intact skin by a transcutaneous power transmitter. To cope in an emergency situation, an emergency power port and emergency outflow clamp subsystem should also be provided.

3.5 Advantages of the Centrifugal Blood Pump

Among the long-term implantable blood pumps, 2 types of clinical needs are clearly exhibited. One is the blood pump utilized as a bridge to transplantation and the bridge to myocardial recovery for cardiomyopathy. If the pump performs effectively and safely for approximately one year or longer, the clinical needs are met by the device. Because an axial flow blood pump is expected to have an operational life of at least 1 year yet the size of the device is extremely small, this device can be offered to practically all the patient population, including females and infants. However, a device which is expected to operate for 2 years or longer is urgently needed. It is becoming clearer that the atherosclerotic regions tend to begin to normalize after monthly lipofiltration or lipoadsorption procedures for at least 2 years. In addition, the need for a permanently implantable pump device is being recognized by many in the health care field. Unfortunately, the current clinically available pulsatile ventricular assist devices are too large to implant in some of the patient population. Two of these pumps are definitely too large to implant intracorporeally for right and left ventricular assistance. However, a centrifugal pump does meet this size requirement. Typically, the centrifugal pump is approximately one-third the size of the pulsatile pump, yet its life expectancy is longer than 5 years. The actuation mode of

pumping is continuous, rather than the energy wasting on and off mode of pulsatile devices. Also, the centrifugal pump is capable of totally unloading the left ventricle and can be operated with an input power of less than 10 W.

Due to high efficiency of the centrifugal pump, a minimum of wasted heat is generated, thus protecting the electronic components and surrounding tissue of the system. Long-term reliable electronic subsystems are assured electrically with a centrifugal pump. In addition, the construction of a centrifugal blood pump is a simple one and does not require trauma and blood clot generating heart valves or a compliance chamber. Its anticipated costs are in the range of one third those of a pulsatile blood pump.

A centrifugal pump consists of an impeller (rotor) driven by a motor or other prime mover, provided with a number of vanes revolving within a stationary casing (stator).The stator is basically a diffuser, that is a passage of increasing flow area, known as a volute. In very large centrifugal pumps the stator may contain internal guide vanes (stationary diffuser) to improve the efficiency of the diffusion process. These two types of centrifugal pumps are illustrated schematically in figure 3.1 below.

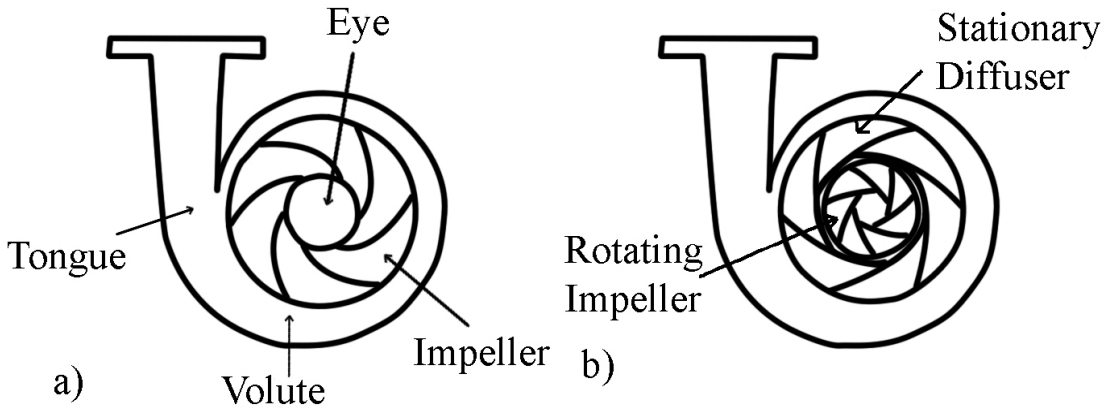

Figure 3.1: Types of Centrifugal Pumps: a) Volute Type b) Diffuser Type

The operation of a centrifugal pump relies on having relative motion between the rotating impeller and the fluid being pumped. The fluid enters axial into the eye of the impeller and is accelerated both outwards (centrifugally) and rotated (tangential or whirl) by the impeller to be discharged with increased velocity and kinetic energy into the diffuser shown in figure 3.1b. In the diffuser the majority of the kinetic energy is converted into pressure energy. The efficiency of the large impeller-diffuser pumps can be greatly increased through these stationary diffuser vanes. However because a centrifugal heart pump is a relatively small pump and the diffuser vanes increase the complexity of the production process and the pump itself, these are not considered to be applicable in this study.

As shown in figure 3.1a, a volute is a curved funnel increasing in area to the discharge port. It is often used with impeller pumps. As the area of the cross-section increases, the volute reduces the speed of the liquid and increases the pressure of the liquid.

3.6 Theory of Centrifugal Pump Design

In figure 3.2, the impeller (rotor) is shown between A and B, provided with a number of vanes and the guide vanes (stationary diffuser) are shown between C and D. The water particles flowing from the suction pipe into the runner at the radius r_1, have a velocity equal to v_1, and the kinetic energy per unit weight of fluid is therefore $v_1^2 / 2g$.

In order that there shall be no shock at entry, the inlet edges of the vanes must make such an angle with tangent to the circle of radius r_1, at the point where the vanes start, that the fluid is sliced by the vanes and not struck [2].

To meet this condition, the angle that the tangent to the first element of the vane must be inclined, with the tangent to the circle of radius r_1, is such an angle β_1 that tan β_1 is equal to the absolute velocity v_1, divided by the peripheral velocity u_1 at radius r_1.

This is shown by the parallelogram of velocities at entrance A in Figure 3.2, w_1 being the relative velocity of the fluid at inlet, that is, the velocity of flow of the fluid along the vane. The fluid then flows through the runner passages (formed by two consecutive vanes from A to B) from entry to exit of runner, leaving with an absolute velocity v_2.

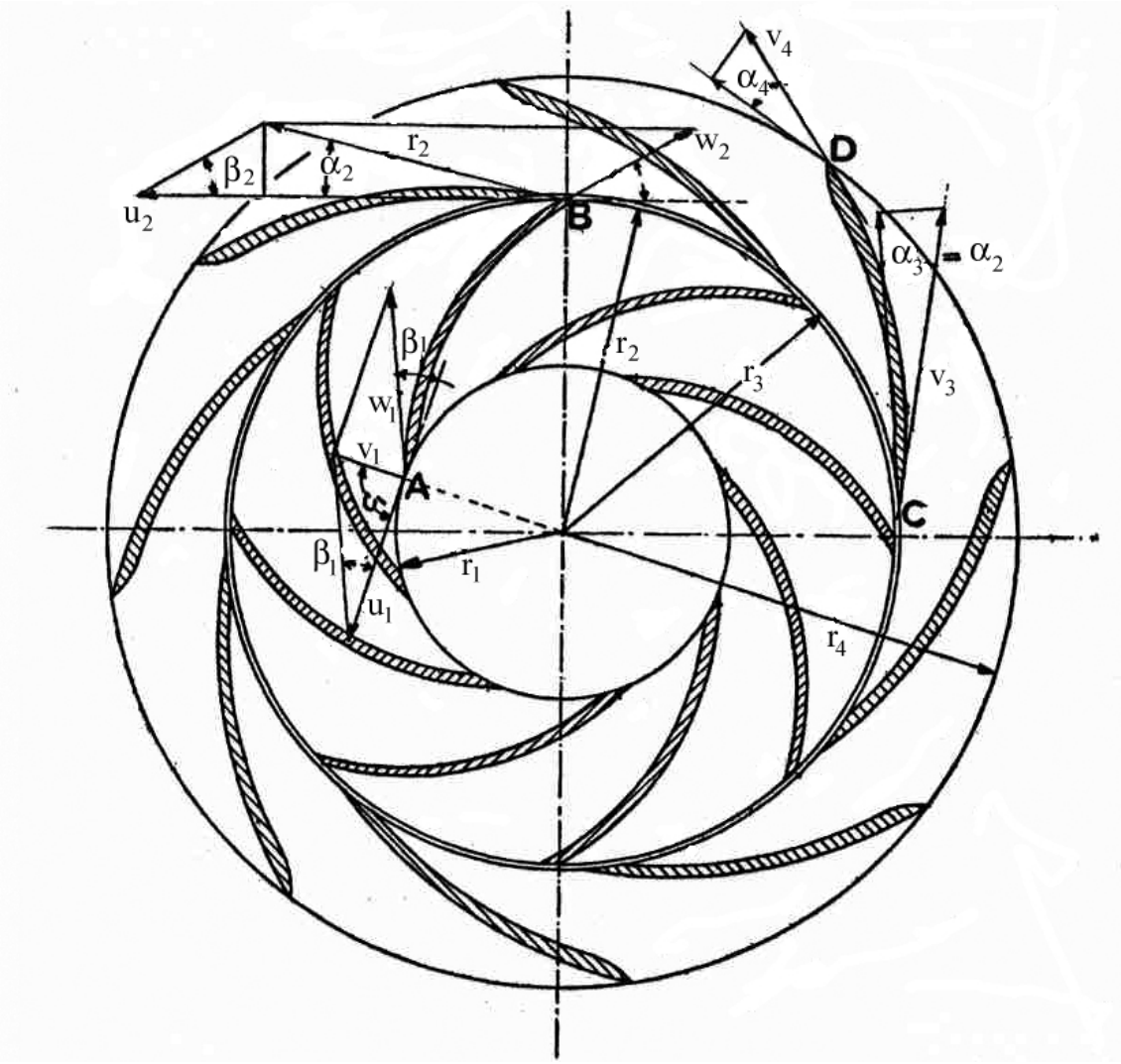

Figure 3.2: Section View of the Impeller [2]

The absolute velocity v_2 is the diagonal of the parallelogram of velocities shown at the B, formed by the peripheral velocity u_2 and the relative velocity w_2 as sides.

On leaving the runner the fluid enters the diffuser provided with guide vanes, so designed that the fluid enters without shock, and during its flow along the passages formed by two consecutive vanes, its velocity is gradually reduced from v_3 at C, to v_4 at D and consequently this reduction of kinetic energy appears as an increase in pressure energy.

From the outlet of the diffuser at D, the fluid flows into and around the casing named as volute, to the discharge pipe, a further increase in pressure energy taking place if the volute is properly designed.

This type of pump has a rather complex design, used with very large sizes and is more expensive to produce than the pump shown in figure 3.1a where the fluid is discharged directly from the impeller into the spiral casing that is volute. This is rather a simple pump to produce and analyze. There are no guide or diffusion vanes to clog up or renew owing to breakage. Therefore in this thesis this volute type centrifugal pump is used as basis of design process.

In order to drive the mathematical formulas of the physics of the centrifugal pumps a general approach will be hold. According to these formulas the design process will be carried out. The basic design relationship for all turbomachines is very simple and is only a form of Newton's Laws of Motion applied to a fluid traversing a rotor [4]. A rotor of a generalized turbomachine is represented in figure 3.3. In this figure o – o is the axis of rotation, and ω is the angular velocity. In the figure 3.3, 1 is where the fluid enters this rotor, then the fluid passes through the rotor by any path and is discharged at 2, the directions of the fluid at 1 and 2 being at any arbitrary angles and points 1 and 2 being at any radii r_1 and r_2. The flow is assumed to be steady flow in the usual thermodynamics sense; that is, the mass rate of flow is constant, the state of the fluid at any given point is constant, and the quantities of heat and work passing in or out of the rotor are constant. Further, the velocity vectors at the inlet and outlet, although acting at points, are regarded as representing the total flow over a finite area, that is, any velocity $V = Q / A$, where Q is

the volume flow rate and A is the cross sectional area normal to the flow. This condition also implies that there is no leakage loss, that is, all the fluid is undergoing the same process.

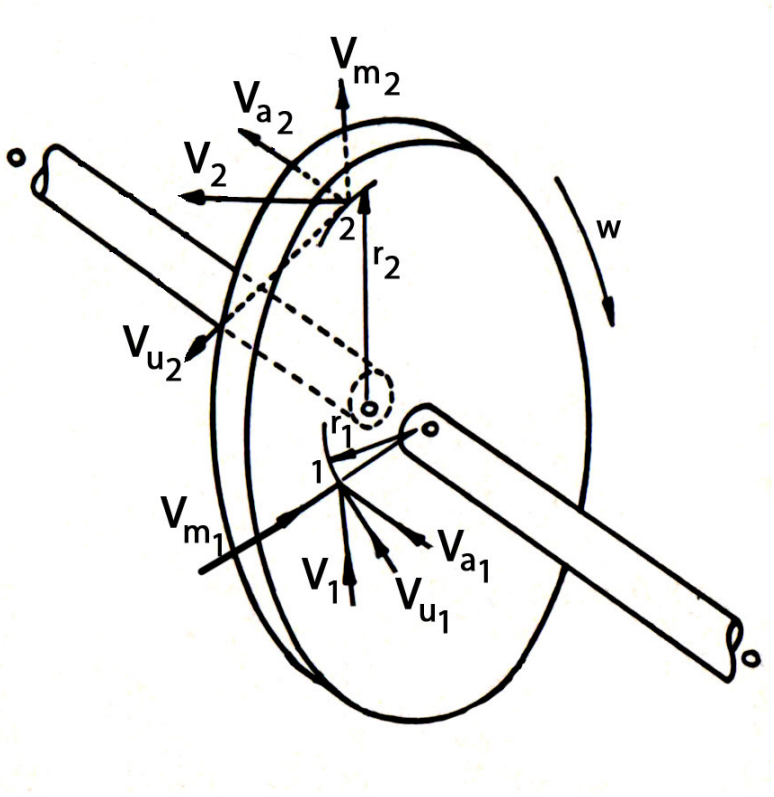

Figure 3.3: Velocity Components for a Generalized Turbomachine [2]

The velocity vectors may be resolved into three mutually perpendicular components as shown in figure 3.3, one directed parallel to the axis of rotation, giving an axial component V_a, one directed radially through the axis of rotation, giving a radial component V_m, and the remaining one in a direction at right angles to the radial direction, giving a tangential component V_u. The change in magnitude of the axial velocity components through the rotor gives rise to an axial force, which must be taken by a thrust bearing to the stationary rotor casing. The change in magnitude of the radial velocity components is carried in a similar

manner as a journal load. Neither has any effect on the angular motion of the rotor. The change in magnitude and of radius of the tangential components of velocity, however, corresponds to a change in angular momentum or moment of momentum of the fluid and by Newton's Laws of Motion is equal to the summation of all the applied forces on the rotor, i.e., the net torque of the rotor τ. This may be expressed in general as follows. If a mass of fluid M_1 enters the rotor at radius r_1, with a tangential component of velocity V_{u1} during time t, and a mass M_2 leaves at radius r_2 with a tangential component of velocity V_{u2} in the same interval of time t, then

$$\tau = \frac{M_1}{gt} r_1 V_{u1} - \frac{M_2}{gt} r_2 V_{u2}$$

For the conditions of steady flow postulated previously, then $M_2 / t = M_1 / t = m$, the rate of mass flow, and the torque exerted by or acting on the rotor will be

$$\tau = \frac{m}{g}\left(r_1 V_{u1} - r_2 V_{u2}\right) \qquad (3.1)$$

The rate of energy transfer, E_o, is the product of torque, and angular velocity of the rotor ω, so

$$\omega r = E_o = \frac{m}{g}\omega\left(r_1 V_{u1} - r_2 V_{u2}\right)$$

with ωr = U, linear velocity of the rotor at radius r, then

$$E_o = \frac{m}{g}\left(U_1 V_{u1} - U_2 V_{u2}\right) \qquad (3.2)$$

If now Eq. 3.2 is taken for unit mass flow, then

$$E_o = E = \frac{1}{g}\left(U_1 V_{u1} - U_2 V_{u2}\right) \qquad (3.3a)$$

where E is the rate of energy transfer per unit mass flow rate. If Eq. 3.2 is divided by the mass flow rate, then

$$\frac{E_o}{m} = H = \frac{1}{g}\left(U_1 V_{u1} - U_2 V_{u2}\right) \qquad (3.3b)$$

where H is the energy transferred per unit mass, or the change of head of the fluid. Both forms of Eq. 3.3 have the same symbols but different units.

Eqs. (3.1), (3.2), and (3.3) are forms of the Euler turbine equation and are the basic relations for all forms of turbomachines, whether they be pumps, compressors or turbines. All the energy transfer between the fluid and rotor must be accounted for by the difference of the two UV_u terms; thus if V_u is the ideal tangential velocity as given by the ideal velocity triangles, then τ, E, or H is the corresponding ideal torque, energy transfer or head. On the other hand, the energy transfer implies a change of angular momentum of the fluid and this must be negative for a pump, with $U_2V_{u2} > U_1V_{u1}$.

3.7 Blade Design of the Impeller

The airfoil geometry is used as the blade geometry on the impeller. This choice depends on the pressure characteristics of the airfoil geometries. Airfoil geometry has the advantage of that it can increase efficiently the pressure even its cross section is small. Because the size and efficiency is one of the biggest criteria, this type of design found to be valuable to examine. This design is unique in this sense, because not such a design is examined before. That is this is the first time that the airfoil geometry is used as a centrifugal pump's blades.

The geometric terms and parameters used to define a blade passage are shown in Figure 3.4. The concave side of the blade is the pressure surface, and the convex side is the suction surface. The fluid's pressure is higher on the pressure than the suction surface, due to the curvature of the blade passage, and the resultant force in the tangential direction caused by the turning of the rotor blades pushes the fluid to flow. The overall size of the blade is defined by the chord c or the axial chord c_a, the blade height or span h, the pitch or spacing s, and the stagger angle γ. The throat is the point of minimum area in the passage. Since the

blade passage is arranged to accelerate the flow, the throat is normally located close to the trailing edge.

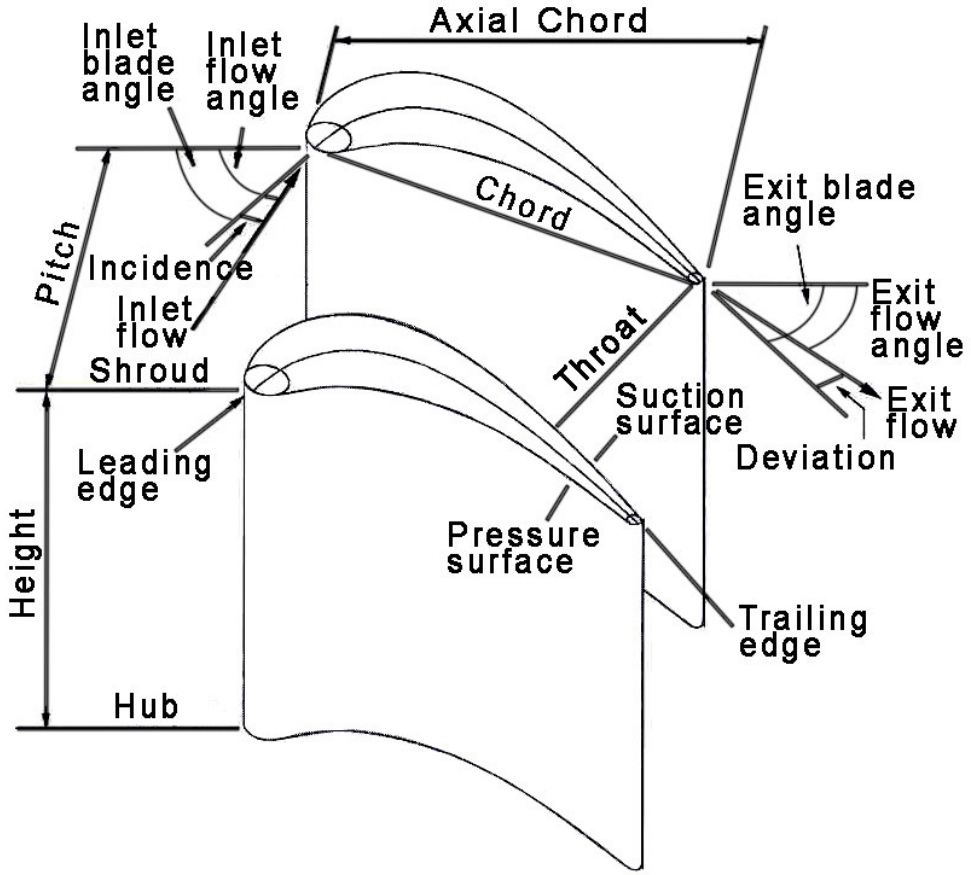

Figure 3.4: Blading Terminology [3]

Various techniques are available for the formation of the airfoil sections, ranging from simple geometric construction, through various standard sections and parametric representations to completely arbitrary geometries that can be manipulated directly on the computer but which retain a high degree of smoothness[3]. A widely used parameterization technique is Pritchard's (1985) technique is also used in this study. In this technique the airfoil is described by the set of eleven parameters listed and shown in Figure 3.5. These

eleven parameters are airfoil radius, axial chord, tangential chord, unguided turning, inlet blade angle, inlet wedge angle, leading edge radius, exit blade angle, trailing edge radius, number of blades and throat. They are both necessary and sufficient to define the airfoil. Some of these have been fixed in the preliminary design, while initial estimates of others were arrived at using the Computational Fluid Dynamics techniques which will be represented in chapter 4. The Pritchard method is capable of generating a wide variety of sections and that created sections are easily modified. This is extremely useful because the choice of parameter values can only be validated by later analysis so that blade section design is almost inevitably an iterative process. Despite these facts, as with any parameterization, there are some aerodynamically valid airfoil sections that it will not handle.

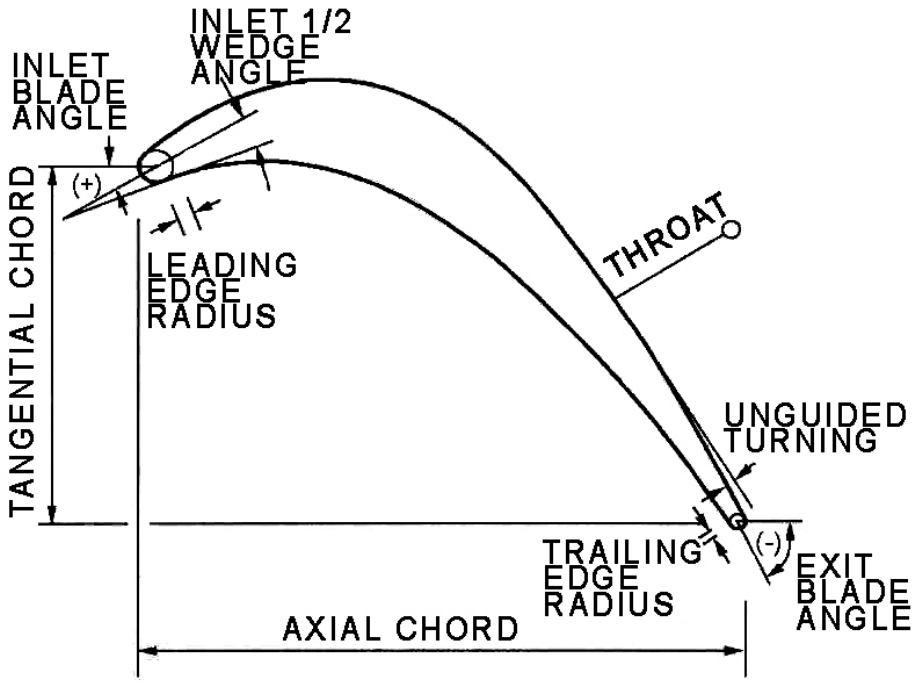

Figure 3.5: Airfoil Geometry and 11 Parameters [3]

In addition to the parameters in Figure 3.5 there are Airfoil Radius and Number of Blades, which are two important parameters used in the definition of airfoil section.

In order to simplify the design process, a commercial software package, named as Bladegen® by ANSYS is used to develop the blade sections. Figure 3.6, shows the dialog of Bladegen® for the input of the angles to define the blade sections.

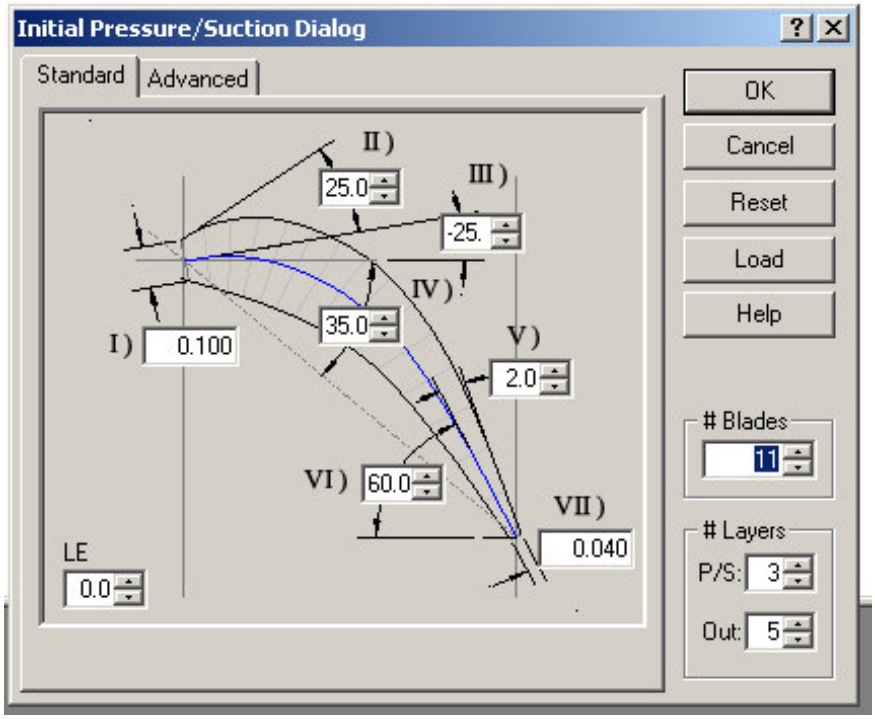

Figure 3.6: Dialog of Bladegen® for the Blade Parameters

3.8 Analysis of a Turbomachine with Radial Flow

In order to understand the effects of the parameters mentioned above, a general analysis of energy transfer will be instructive. It is obvious, that there are too many variables to take them all into account; therefore the analysis will deal with the effect of one major variable only, the fluid discharge angle. The conditions for this illustrative example are chosen as $U_2 = 2U_1$, radial velocity constant, no inlet angular momentum, and an inlet fluid angle of

45°, so that $V_{m1} = V_1 = U_1 = V_{m2}$. The outlet fluid angle, parameter 6, symbolized as β_2 (taken the same as the outlet blade angle) is variable. Figure 3.7, shows the velocity diagrams for these conditions, which are arbitrary but which do not impose severe restrictions on the generality of the analysis for the purpose of this discussion.

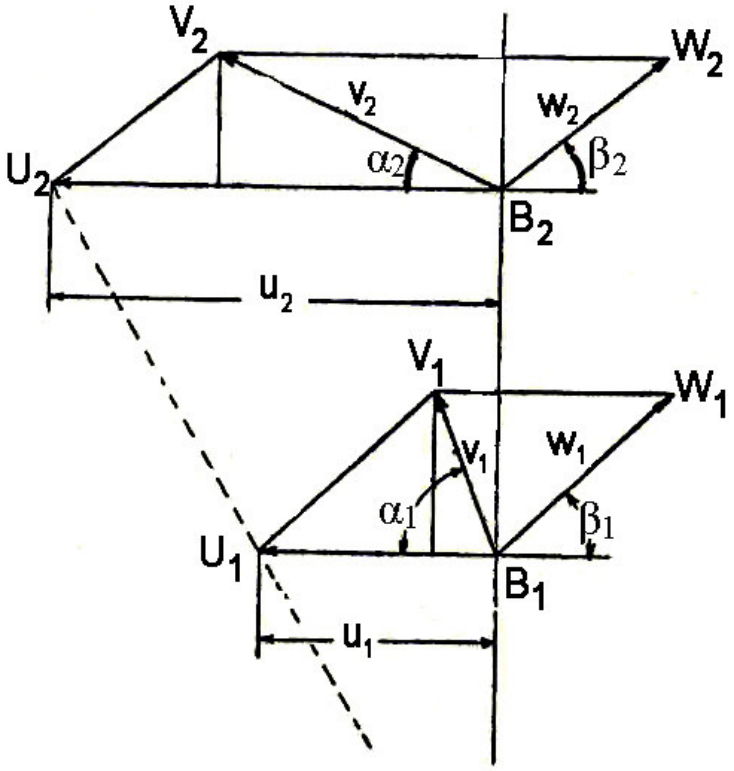

Figure 3.7: Velocity Diagrams for Generalized Radial Flow Turbomachine

As there is no inlet whirl, the energy transfer by Eq. (3.3) becomes

$$E = -\frac{U_2 V_{u2}}{g}$$

which in terms of the radial velocity V_m and discharge angle β_2 becomes

$$E = -\frac{U_2}{g}\left(U_2 - V_m \cot \beta_2\right)$$

and since $U_2 = 2U_1 = 2V_m$ we have $E = \frac{2V_m^2}{g}(\cot\beta_2 - 2)$.

For the purpose of comparison, the term $\frac{V_m^2}{g}$ will be taken as unity so $E = 2(\cot\beta_2 - 2)$

With this simple form for E, values can be plotted with β_2 ranging from very small values through 90° to very large values. The results are shown in figure 3.8.

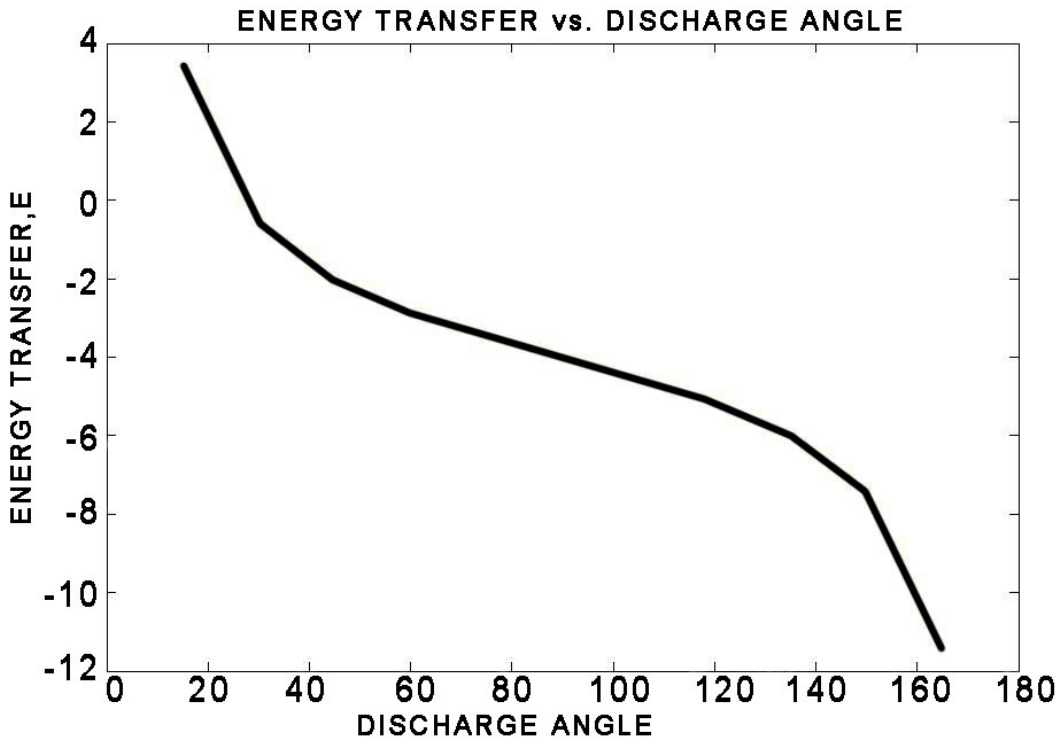

Figure 3.8: Energy Transfer for Generalized Turbomachine

By examining the change of energy transfer with β_2, it will be seen that for discharge angles greater than about 30°, E is negative and increases continually with increasing β_2. By the sign convention, negative values of E imply work done on the fluid and therefore the machine is acting as a pump or compressor. In figure 3.9, velocity diagrams for a few selected values of β_2 are shown and it will be obvious that as β_2 increases so does the value

of V_{u2}, hence the magnitude of E increases. However, for β_2 approximately equal to 26,5°, E becomes zero and from the velocity diagram it will be seen that there is no outlet whirl and $V_1 = V_2$, so the increase of static head due to centrifugal effect must be exactly counterbalanced by the decrease of static head due to increase of relative velocity.

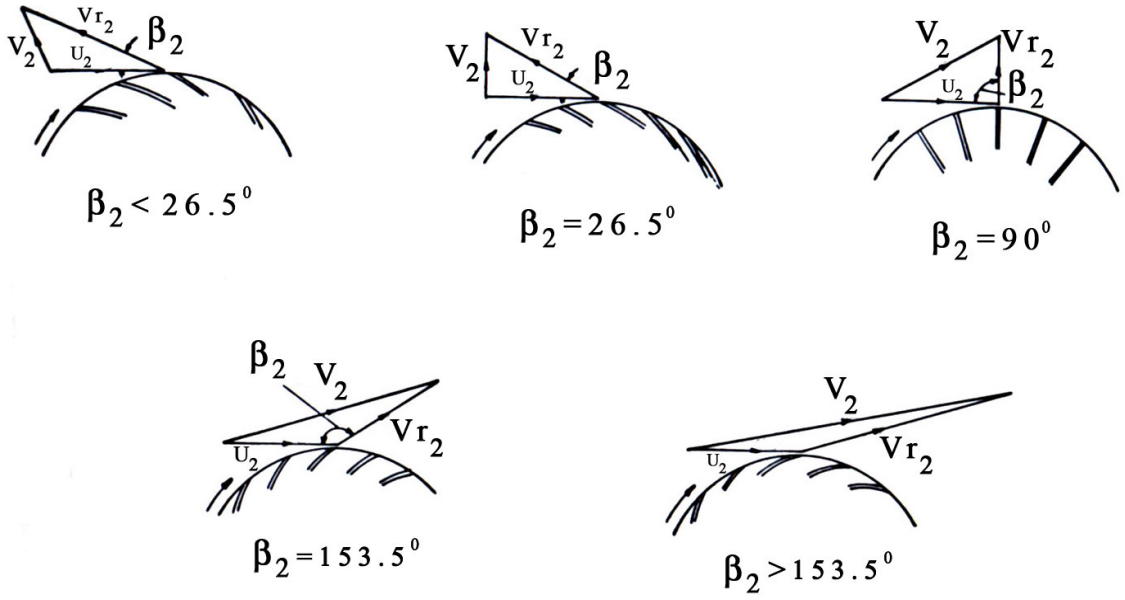

Figure 3.9: Velocity Angles for Various Outlet Blade Angles β_2 [2]

For $\beta_2 < 26,5°$, E is positive and the machine is acting as a turbine. Again the velocity diagram shows this to be so by the whirl component now being in the other quadrant opposite to the direction of rotation. On the other hand, the velocity diagrams show that as β_2 increases, V_2 increases likewise, meaning a greater proportion of energy as discharge kinetic energy and therefore less change of static head. This result is also obtained with the Computational Fluid Dynamics method. These results will be represented in the coming sections. So the outlet blade angle should be taken above 30° as much as it does not destroy

the increase of the head of the pump. This is the basis of the design of the produced impellers (named as models 13&16 mentioned in next section).

3.9 Blade Design Process

As stated before, by using Bladegen® by keeping parameters 1,5 and 7 constant and changing parameters 2,3,4 and 6 from figure 3.6, 17 impeller models are designed. The values of the parameters are listed in table 3.1.

Model No	**Param. #1**	**Param. #2**	**Param. #3**	**Param. #4**	**Param. #5**	**Param. #6**	**Param. #7**
1	0.1	**15**	-25	35	2.0	60	0.04
2	0.1	**20**	-25	35	2.0	60	0.04
3	0.1	**30**	-25	35	2.0	60	0.04
4	0.1	**35**	-25	35	2.0	60	0.04
5	0.1	25	**-15**	35	2.0	60	0.04
6	0.1	25	**-20**	35	2.0	60	0.04
7	0.1	25	**-30**	35	2.0	60	0.04
8	0.1	25	**-35**	35	2.0	60	0.04
9	0.1	25	-25	**25**	2.0	60	0.04
10	0.1	25	-25	**30**	2.0	60	0.04
11	0.1	25	-25	**40**	2.0	60	0.04
12	0.1	25	-25	**45**	2.0	60	0.04
13	0.1	25	-25	35	2.0	**50**	0.04
14	0.1	25	-25	35	2.0	**55**	0.04
15	0.1	25	-25	35	2.0	**65**	0.04
16	0.1	25	-25	35	2.0	**75**	0.04
17	0.1	25	-25	35	2.0	60	0.04

Table 3.1: Values of the Changing Parameters

The performances of these pumps are predicted by using computational fluid dynamic techniques. Model 13 gives the highest pressure head, so the production process was focused on this model and also model 16 is produced and tested. The results of Computational Fluid Dynamics and performance specifications of these pumps will be presented in chapter 4 and 5.

3.10 Volute Design

The function of the casing which receives the fluid from the impeller is two fold: (1) to receive the fluid discharged from the complete periphery of the impeller and to guide it with minimum loss into one or more outlet ports, and (2) to reduce the high absolute velocity at the impeller tip in order to convert the kinetic energy to static head or pressure. This may be described as a collector function and a diffuser function. Collecting and diffusing may be done separately or together and one may precede or follow the other.

This collector takes the form of a volute or scroll as shown in figure 3.10. Their advantage is their simplicity and low cost. The volute consists of a casing surrounding the impeller, gradually increasing in cross-sectional area from the tongue to the throat and may be regarded as a straight tapered duct wrapped around the impeller periphery. It will be noticed that the tongue is actually given some initial radial clearance which is necessary to smooth out the flow to avoid excessive turbulence and noise. There is some recirculation on this gap and too large a clearance leads to reduced efficiency.

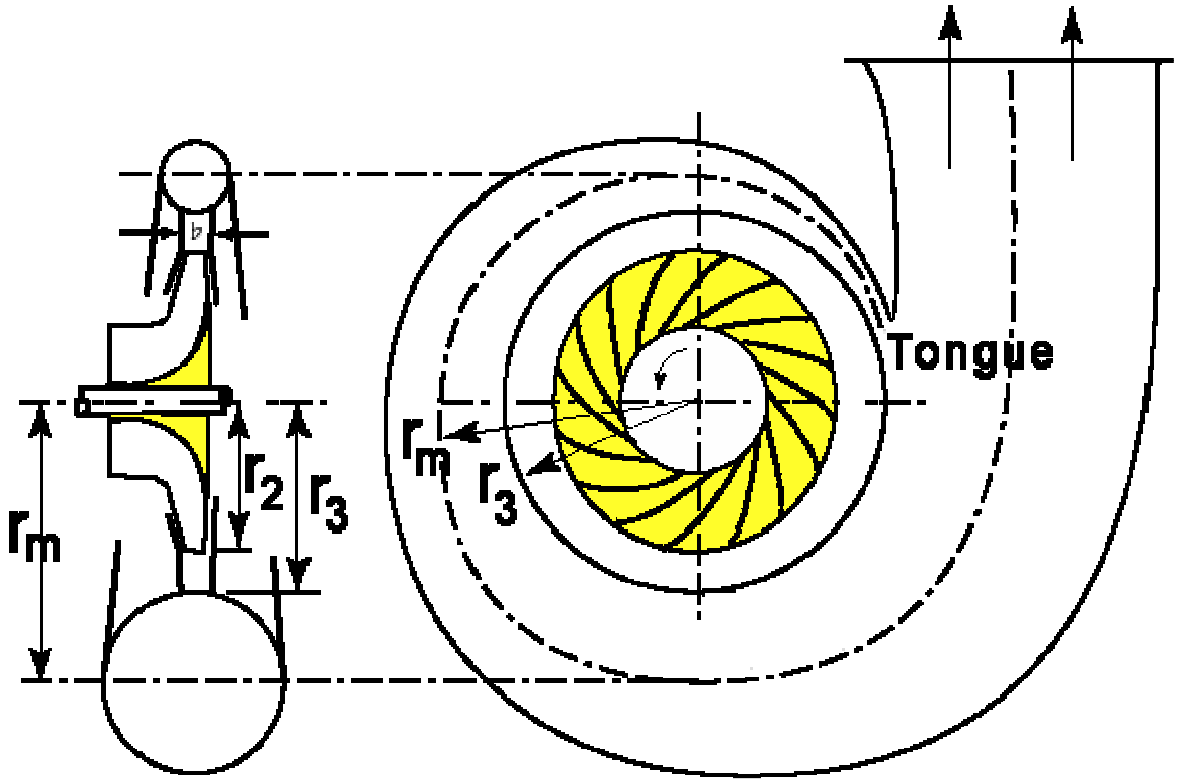

Figure 3.10: Volute Design Parameters

The parameters of the designed volute are as follows: r_2 = 24.15mm, r_3 = 24.30mm and r_m = 29.30mm.

Chapter 4

COMPUTATIONAL FLUID DYNAMICS

4.1 Introduction

Computer based numerical flow and mass transport simulation tools, such as computational fluid dynamics (CFD), can provide detailed, three dimensional predictions of fluid flow and mass transport in complex geometries. Commercially available, general purpose CFD softwares, such as ANSYS Advanced CFD®, Fluent® and CosmoFloworks® , are used routinely as a design tool in the aerospace, automotive, and process industries and also has been applied to predict the flows and mass transfer in various medical devices.

The physical aspects of transport phenomena in the macroscale are governed by fundamental principles of mass, momentum, and energy conservation expressed in terms of algebraic equations, ordinary/partial differential equations, or integral representations. Numerical simulation is the technique of replacing the transport equations with algebraic equations and obtaining a final numerical description of the phenomenon in time and/or space domain. These simulation techniques and their applications to complex design projects are related intimately to the advancement in computer technology fulfilling the increasing demand for speed and storage required by the numerical simulation of the flow and mass transport problems in artificial organ design.

CFD techniques and principles are applicable and valuable in the development of any blood contacting medical device with demanding performance and reliability requirements, including bioprosthetic and flexible synthetic heart valves, blood pumps, stents, grafts, blood access and purification devices, and others. Used at appropriate stages of the design cycle, ideally, integrated with other computational tools such as finite-element stress analysis, CFD offers a detailed understanding of fluid mechanics that complements the clinical, technical, and experimental experience of the design team.

A major benefit offered by CFD is the ability to evaluate designs quickly at an early stage, before committing to the expense of prototype manufacture and testing. Therefore CFD can reduce the costs, time scales, and risks associated with development of a new design.

At the detailed design stage, CFD can investigate quickly the effects of design changes on blood flow to reduce the risk of unexpected knock-on effects that otherwise would become apparent only at a later stage. When a final design has been reached, CFD analysis can be used to confirm that design goals have been achieved. The detailed CFD picture of the flow field can be used often to support and explain experimental results, potentially strengthening regulatory submissions and providing a scientific base for clinical use.

There is a strong relationship between the mechanical loading on blood cells and their trauma. Foreign material interaction and flow induced mechanical damage are the main issues of hemolysis in artificial organs besides thermal, chemical, and osmotic effects. An integrative analysis of its biocompatibility requires CFD, the validation with flow visualization, and comparison with hemolysis tests results. In vitro hemolysis test require experimental effort and quite a number of repetitions due to the large statistical variations. A computational assessment or quantification of shear-induced hemolysis in the design phase of artificial organs decreases the effort and cost of design and aids development, as clearly proven for the design of rotary blood pumps.

4.2 Turbulence Model

The flow in the blood pump is highly disturbed because of the moving blades; therefore the flow pattern in most regions inside the blood pump is turbulent [5]. It is important to choose the turbulence models for the CFD simulation. However, which turbulence model is appropriate for miniature blood pump is not obvious. The assumptions of turbulence models have to be reevaluated for the specific application of small-size blood pumps. On the other hand, the complicated geometry of blood pump and relatively low absolute speed makes wall effects more strongly influence the flow field. There are different treatments of near-wall regions, which should be chosen carefully in order to make them compatible with turbulence models. This is critical for accuracy and feasibility of CFD prediction.

In this study, commercially available CFD packages Fluent® and Cosmos Floworks® are used to optimize the design of the centrifugal blood pump. As an appropriate and validated solver, a turbulent flow model is chosen. The turbulence model chosen is k-ε model. Here k denotes the turbulent kinetic energy, and ε denotes the turbulent dissipation rate. This model utilizes the eddy viscosity assumption to relate the Reynolds stress and turbulent terms to the mean flow variables. The k – ε model is the most popular two – equation model [8]. The near wall treatment includes standard wall functions, Non-Equilibrium wall functions and enhanced wall treatment. In this study because of the blade geometry and the rotation the non-equilibrium wall functions are chosen. The fluid is water-liquid as used in the experiments. The density of the water-liquid is 998.2 kg/m^3 and the viscosity is 0.001003 kg/m-s. The Pressure-Velocity Coupling is chosen as SIMPLE. The discretization methods are Standard for Pressure, and Second Order Upwind for Momentum, Turbulence Kinetic Energy and Turbulence Dissipation Rate. The solver type is Segregated, formulation is Implicit and the state is Steady.

k – ε turbulence model includes the standard k – ε model, the renormalization group (RNG) k – ε model and the realizable k – ε model. It is proven that all these three models

are suitable for the numerical simulation of the internal flow inside a centrifugal pump [6]. Also with the same study it is shown that the result of the numerical simulation from the Realizable k – ε model agrees with the experimental result in a best way. Therefore in our study as the Realizable k – ε model is used for the solver type.

4.3 Basic Equations

For three dimensional incompressible flow, the continuity and the momentum Navier – Stokes equations in the rotating coordinate systems can be written as follows:

$$\frac{\partial \rho}{\partial t} + \frac{\partial (\rho u_j)}{\partial x_j} = 0$$

$$\frac{\partial (\rho u_i)}{\partial t} + \frac{\partial (\rho u_j u_i)}{\partial x_j} = \frac{\partial \left[\mu_e \left(\frac{\partial u_i}{\partial x_j} + \frac{\partial u_j}{\partial x_i} \right) \right]}{\partial x_j} - \frac{\partial P}{\partial x_i} + S_i$$

The stated equations are improved with the k – ε turbulence model. It introduces two transport equations: one is the turbulence kinetic energy k, the other is the dissipation rate ε. The realizable k – ε turbulence model is developed by Shih et al.[7] It is a relatively recent development and contains a new eddy-viscosity formula involving a variable C_μ originally proposed by Reynolds and guaranteeing the reliability of the model, and a new transport equation for the dissipation rate, ε, based on the dynamic equation of the mean-square vorticity fluctuation.

Its transport equations for “k” and “ε” are described as follows:

$$\frac{\partial (\rho k)}{\partial t} + \frac{\partial (\rho k u_j)}{\partial x_j} = \frac{\partial}{\partial x_j} \left[\left(\mu + \frac{\mu_t}{\sigma_k} \right) \frac{\partial k}{\partial x_j} \right] + \rho (P_k - \varepsilon)$$

$$\frac{\partial (\rho \varepsilon)}{\partial t} + \frac{\partial (\rho \varepsilon u_j)}{\partial x_j} = \frac{\partial}{\partial x_j} \left[\left(\mu + \frac{\mu_t}{\sigma_\varepsilon} \right) \frac{\partial \varepsilon}{\partial x_j} \right] + \rho C_1 E \varepsilon - \rho C_2 \frac{\varepsilon^2}{k + \sqrt{\upsilon \varepsilon}}$$

where

$$C_1 = \max\left(0.43, \frac{\eta}{\eta+5}\right)$$

$$C_\mu = 1/A_0 + A_S U^* k/\varepsilon$$

$$A_s = \sqrt{6}\cos\phi$$

$$\phi = \frac{1}{3}\cos^{-1}\left(\sqrt{6}W\right)$$

$$W = E_{ij}E_{jk}E_{ki}/\left(E_{ij}E_{ij}\right)^{1/2}$$

$$U^* = \sqrt{E_{ij}E_{ij} + \Omega'_{ij}\Omega'_{ij}}$$

$$\Omega'_{ij} = \Omega_{ij} - 2\varepsilon_{ijk}\omega_k$$

$$\Omega_{ij} = \overline{\Omega_{ij}} - \varepsilon_{ijk}\omega_k$$

The model constants are $\sigma_\varepsilon = 1.2$, $C_2 = 1.92$ and $A_0 = 4.0$.

4.4 Computational Grid and Method

The geometry of the pump is composed of inlet zone, outlet zone, impeller and volute. FLUENT uses the finite volume method and the 3D Navier-Stokes equations are solved. The grids of the impeller, volute and inlet pipe are generated as three different volumes. Unstructured tetrahedral cells are generated to define the impeller which formed 416042 mesh volumes. This generated grid is presented in figure 4.1 and 4.2. For the inlet pipe, hexcore tetrahedral cells of size 1 are generated, which resulted in 256104 cells. Figure 4.3 and 4.4 present the grid for the inlet pipe. For the volute part, unstructured tetrahedral cells are used with the size of 0.5 and this resulted in 394211 cells. The generated grid for the volute is shown in figure 4.5 and 4.6.

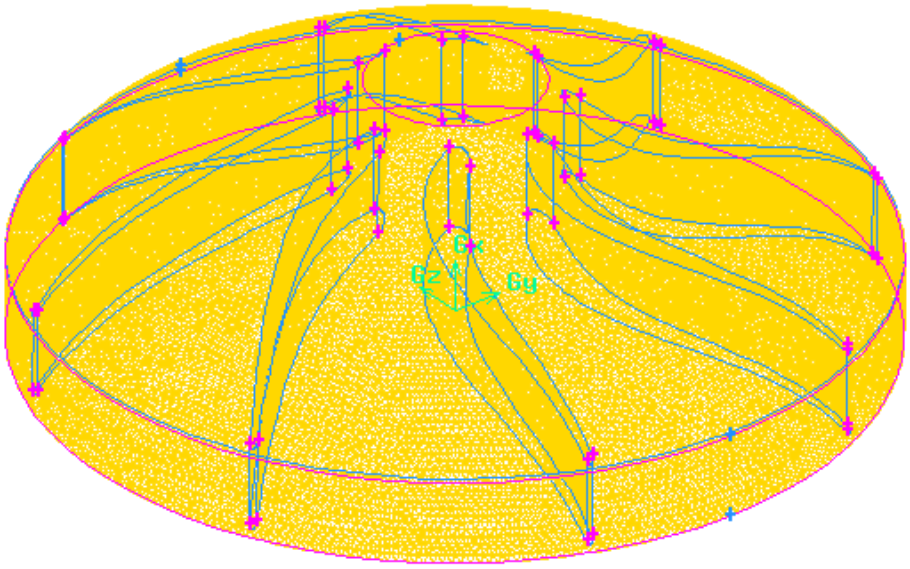

Figure 4.1: Mesh of the Impeller

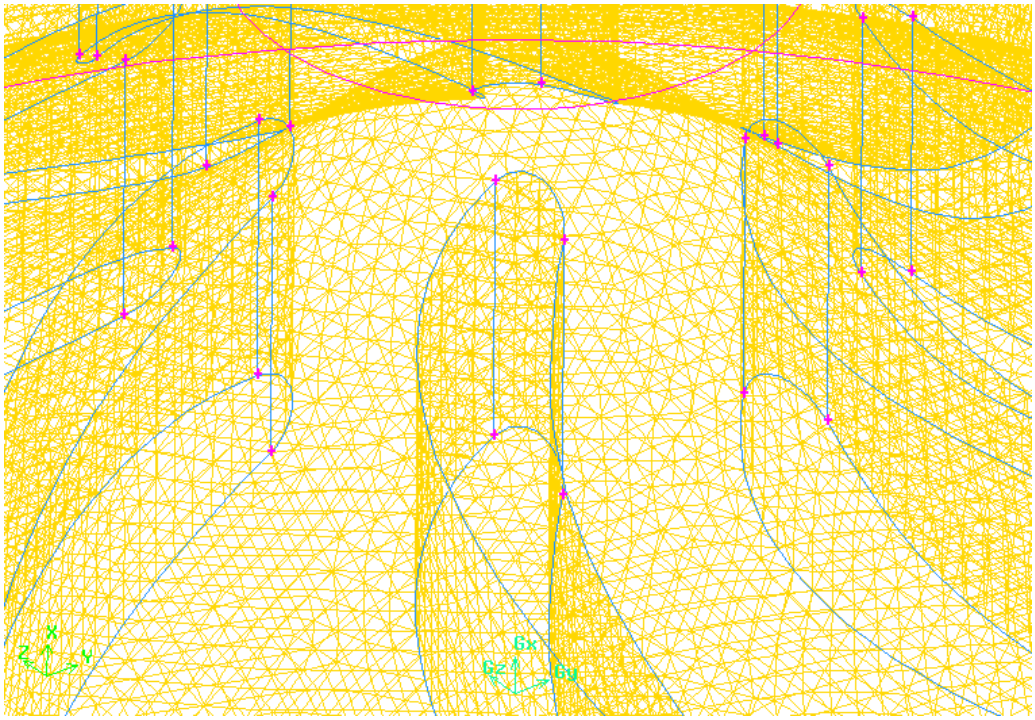

Figure 4.2: Detailed View of the Mesh of the Impeller

Figure 4.3: Mesh of the Inlet Pipe

Figure 4.4: Detailed View of the Mesh of the Inlet Pipe

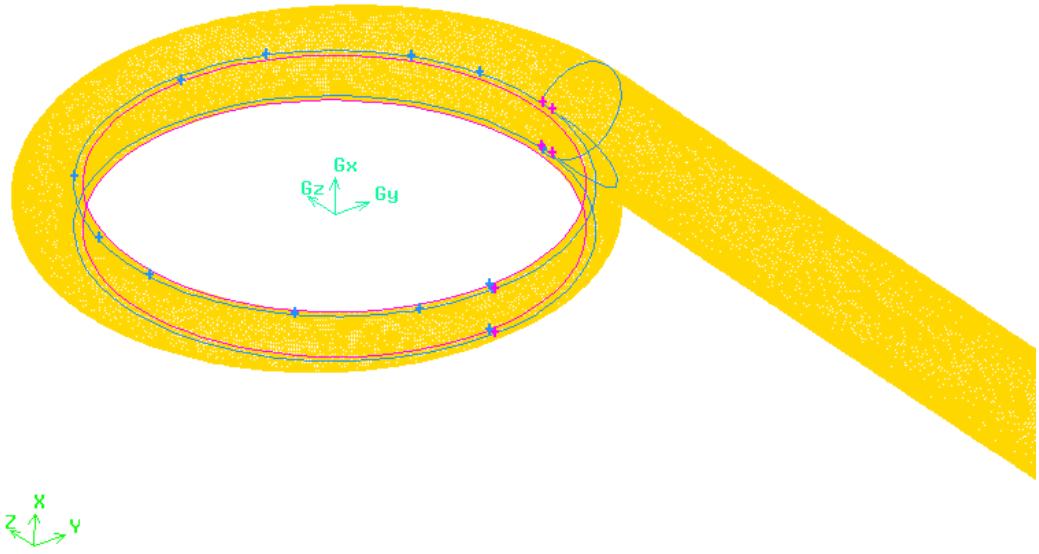

Figure 4.5: Mesh of the Volute

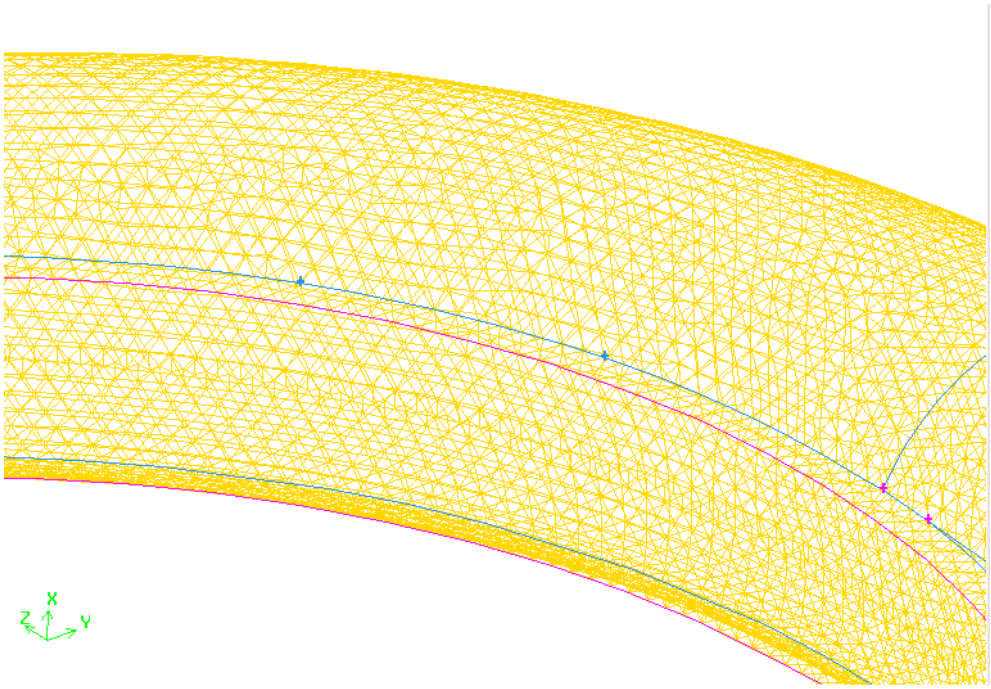

Figure 4.6: Detailed View of the Mesh of the Volute

Chapter 5

APPLICATIONS & RESULTS

5.1 Introduction

Chapter 3 and chapter 4 presented the theory of the design and the theoretical prediction of the performance curves. In this chapter the computational fluid dynamics results for the blade geometries, manufacturing process of the chosen impellers, experimental setup and results will be presented.

5.2 Computational Fluid Dynamics (CFD) Results

CFD is used first in the comparison of the different impeller designs. The mentioned 17 different designs were simulated. Those promised the best performances are produced and tested. Secondly CFD is used to compare the experimental results and the theoretical predictions for the produced impeller.

Comparison of the Impellers

In order to compare the performances of the designed impellers, computational fluid dynamics methods are used. All of the impellers are simulated with the same inlet and outlet conditions of the pump. Also the volute geometry and inlet pipe is the same in every simulation. Table 5.1 shows the performance prediction of the designed 17 impeller

geometries. For these simulations the rotational speed of the impeller is kept at 2000rpm, the inlet pressure at 0 Pa, the outlet pressure at environmental pressure which is 101325 Pa, and the flow rate at 5 L/min.

Model No:	**Calculated ΔP (Pa)**	**Calculated ΔP (mmHg)**	**Parameter & Value**
1	14000	105	Parameter 2: 15
2	15000	112,5	Parameter 2: 20
3	14000	105	Parameter 2: 30
4	14000	105	Parameter 2: 35
5	14000	105	Parameter 3: -15
6	14500	108,75	Parameter 3: -20
7	15000	112,5	Parameter 3: -30
8	13000	97,5	Parameter 3: -35
9	11000	82,5	Parameter 4: 25
10	13000	97,5	Parameter 4: 30
11	13600	102	Parameter 4: 40
12	13000	97,5	Parameter 4: 45
13	16500	123,75	Parameter 6: 50
14	14400	108	Parameter 6: 55
15	14200	106,5	Parameter 6: 65
16	14400	108	Parameter 6: 75
17	14300	107,25	Default parameters

Table 5.1: CFD Prediction of the Impeller Performances

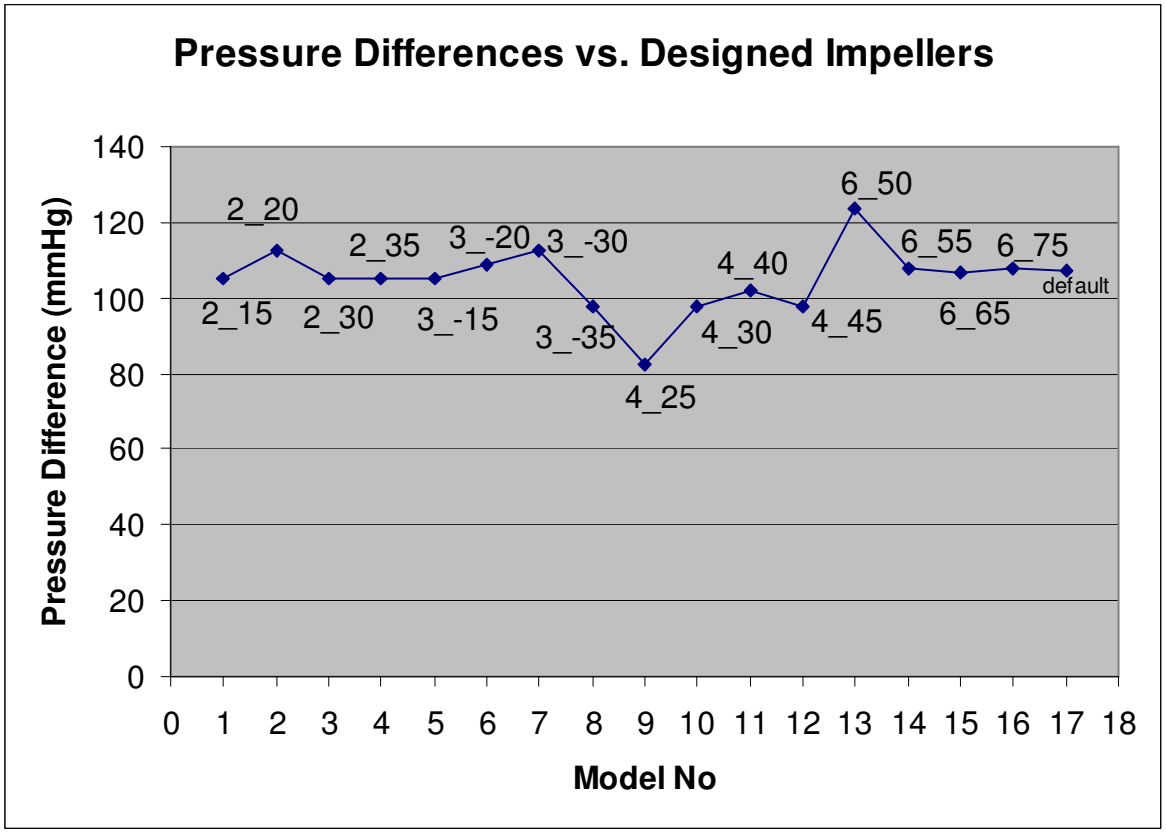

Figure 5.1: CFD Prediction of the Impeller Performances

For a better understanding the performance comparison is shown with figure 5.1. From the results it is seen that the model 13 gives the best performance in terms of the pressure rise. It can be also understood from the results, for the second parameter the best performance is achieved at the value of 20. On the other hand it is seen from the graph that increases beyond this value decreases the performance of the impeller. The best performance for the third parameter is achieved at -30. Also for this parameter beyond this value the performance decreases suddenly. The fourth parameter gives the best performance at the value of 40. The values below 40 give poor performances. As the last

variable, sixth parameter gives the best performance at 50. According to these results impeller models of 16 and 13 are produced and tested.

5.3 Production and Tests of Models 16 and 13

5.3.1 Model 16

As the first production model 16 is chosen. The design is carried out with CAD systems and CAM module of Unigraphics® is used to generate its CNC codes. It is produced with 3-axis CNC milling machine at the Manufacturing Automation Research Center.

The pump consists of the casing and the impeller. Figure 5.2 shows the CAD model of the impeller of model 16.

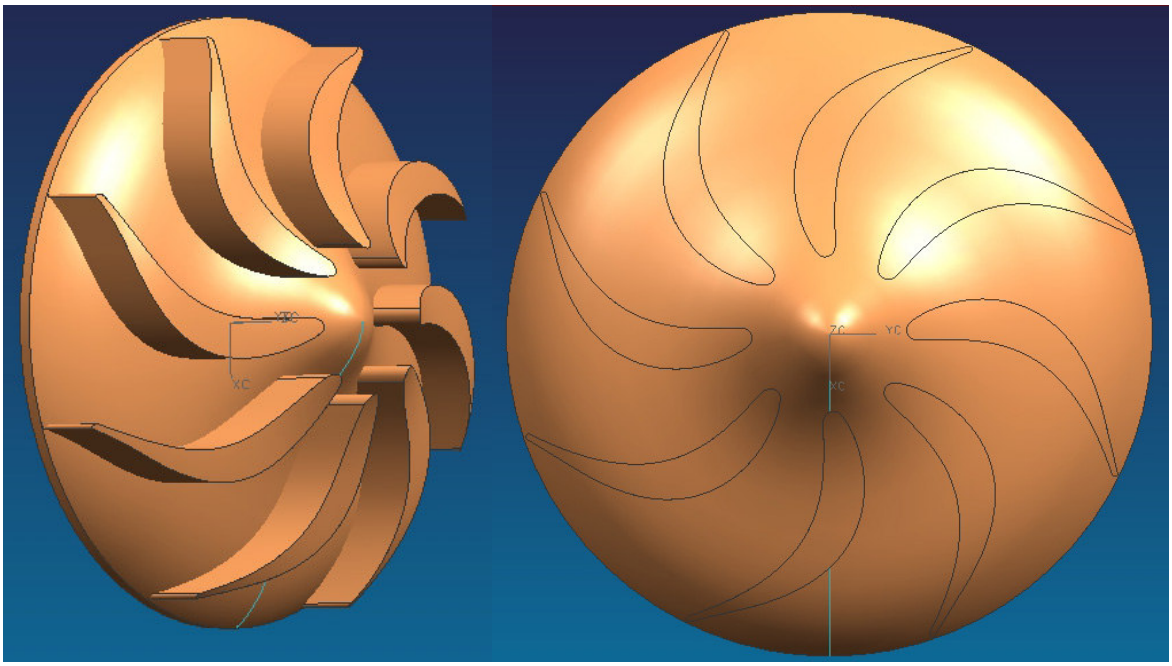

Figure 5.2: CAD model of the Impeller geometry of the model 16

Figure 5.3 shows the CAD model of the upper casing of the pump.

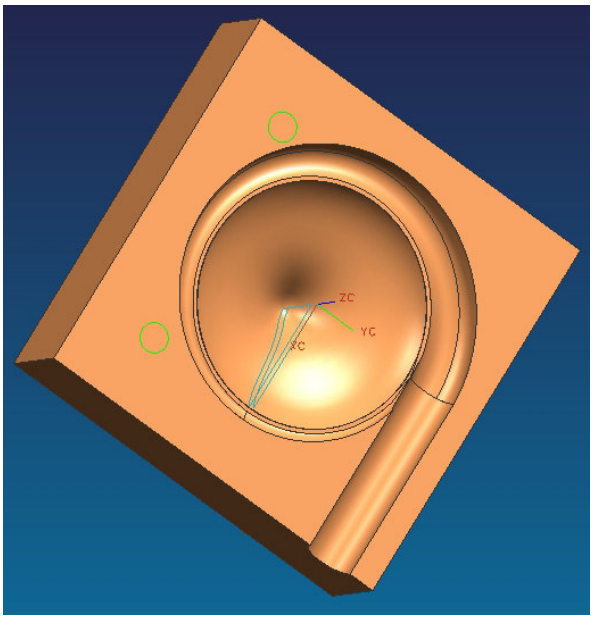

Figure 5.3: CAD model of the upper casing of the pump

Figure 5.4 shows the CAD model of the lower casing of the pump.

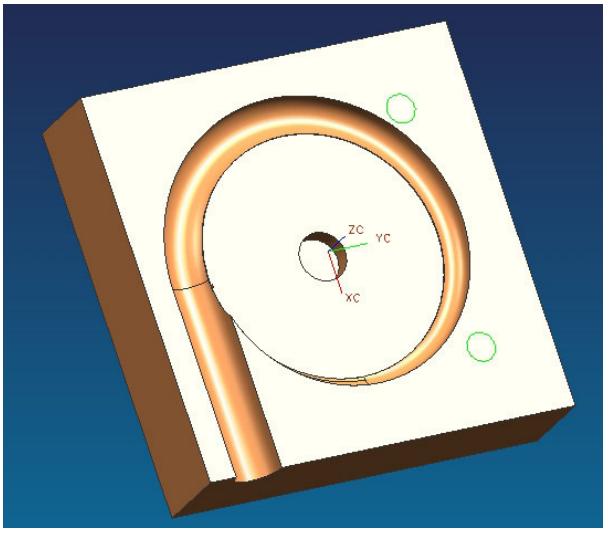

Figure 5.4: CAD model of the lower casing of the pump

After CAD and CAM process the pump is produced. Figure 5.5 shows the produced impeller and the lower casing.

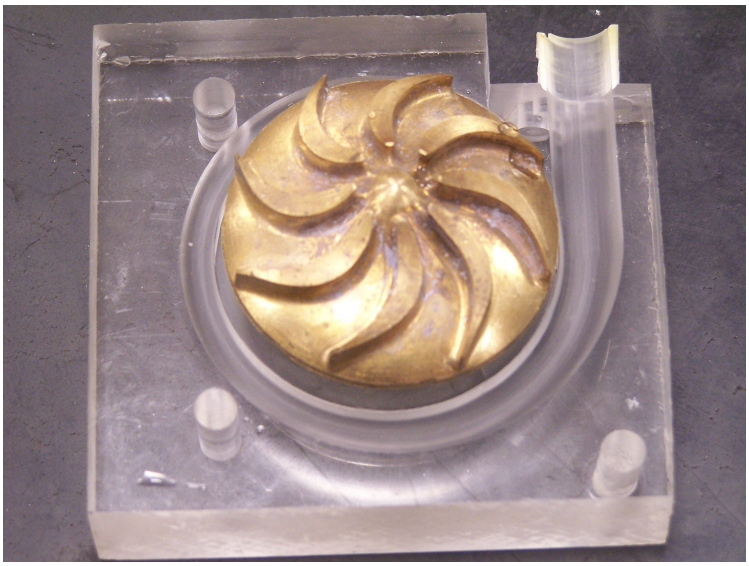

Figure 5.5: Produced Impeller Model 16 and the Lower Casing

Figure 5.6 shows the produced upper casing.

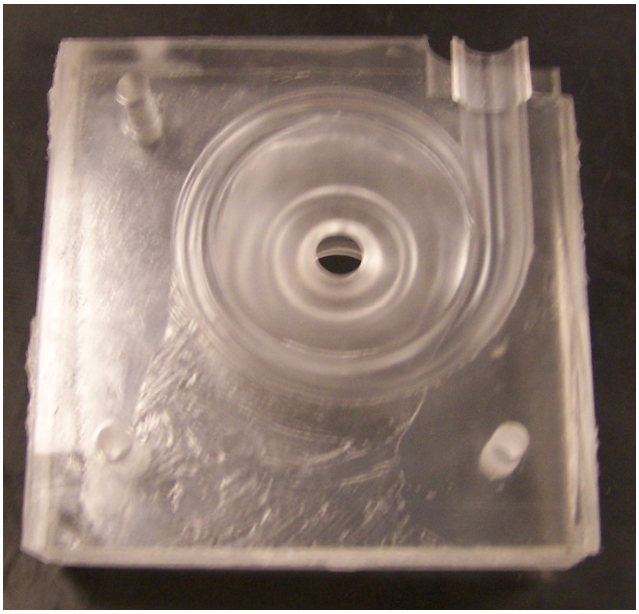

Figure 5.6: Produced Upper Casing

After the production process the pump is formed. The upper casing and lower casing is connected with impeller in between. The impeller is connected to a servo motor through the shaft under it and a bearing is used in the middle of the lower casing. The flow rate and the pressure difference between the inlet and the outlet are measured for four different rotational speeds, which are 500, 1000, 1500 and 2000 rpm. Figure 5.7 shows the pump and the driving servo motor.

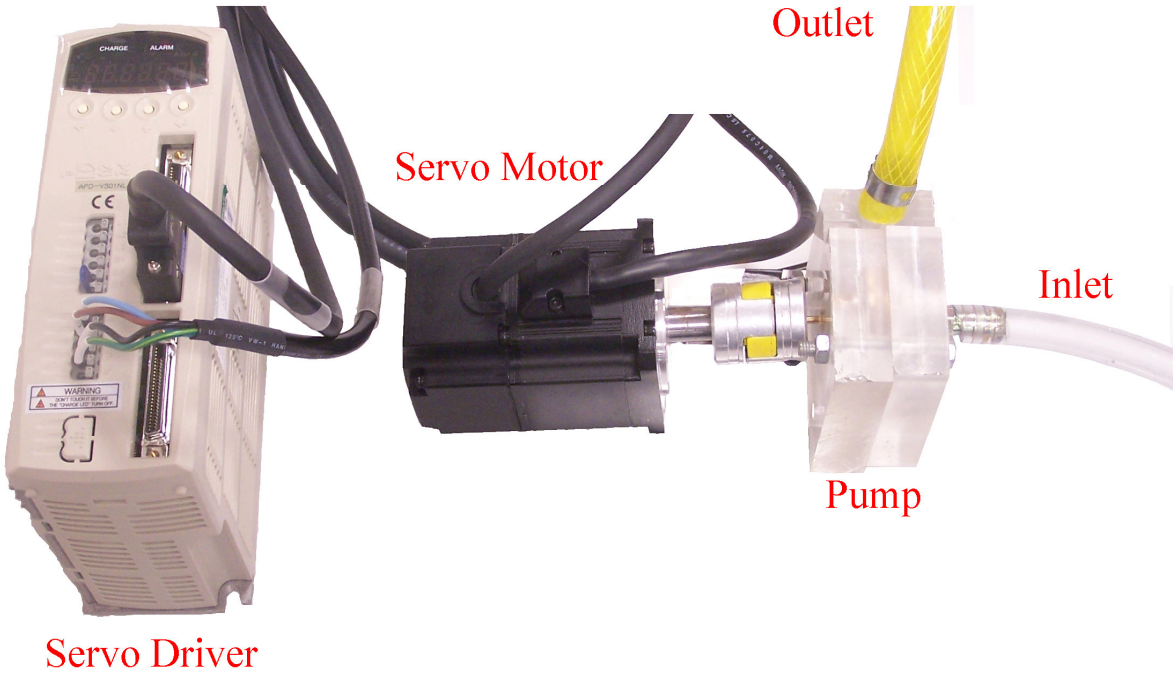

Figure 5.7: Pump and Driving Mechanism

Here the servo motor drives the impeller and the flow passes from inlet to the outlet. The servo driver is used to arrange the rotational speed of the impeller.

Table 5.2 shows the experimental results and CFD results. Here the measured pressure difference between inlet and outlet and the flow rate is presented. The measured data is supported with the theoretical prediction of the CFD techniques.

Rotational Speed (rpm)	Measured ΔP (mmHg)	Calculated ΔP (mmHg)	Flow Rate (L/min)
500	8,09	5,16	0,9
1000	31,63	22,07	2,172
1500	72,83	50,02	3,252
2000	110,34	106,66	4,308

Table 5.2: Experimental and Computational Results for Model 16

Figure 5.8 shows these experimental and computational results as a graph for a better comparison.

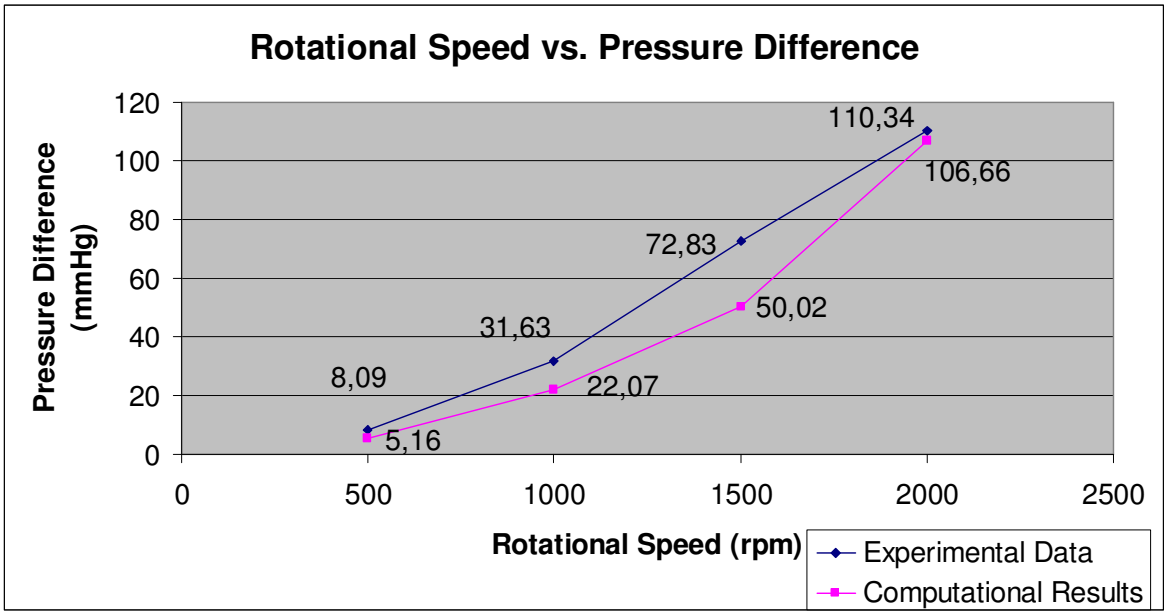

Figure 5.8: Graph of Experimental and Computational Results

As it is seen from figure 5.8, the theoretical and experimental results are in good agreement. For intermediate velocities computational techniques underestimate the pressure difference, but for the upper and lower limits the values are in good agreement.

This underestimation occurs because of the turbulence model in CFD. These types of simulations give results under the experimental results.

The CFD package Fluent can give the pressure contours around the flow volume. Figure 5.9, 5.10, 5.11 and 5.12 show the pressure distributions for speeds 500rpm, 1000rpm, 1500rpm, and 2000rpm respectively.

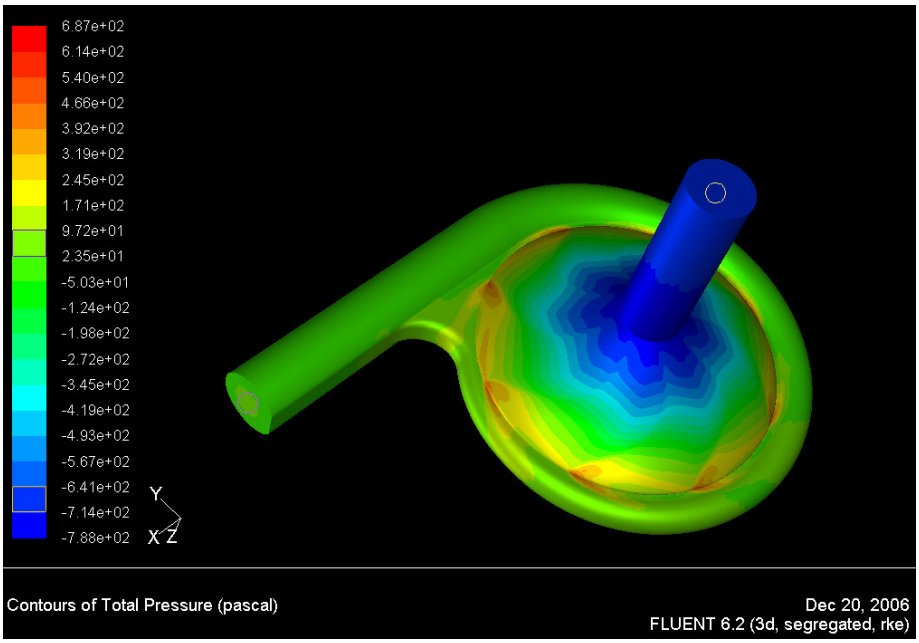

Figure 5.9: Pressure Distribution for Model 16 at Rotational Speed of 500 rpm

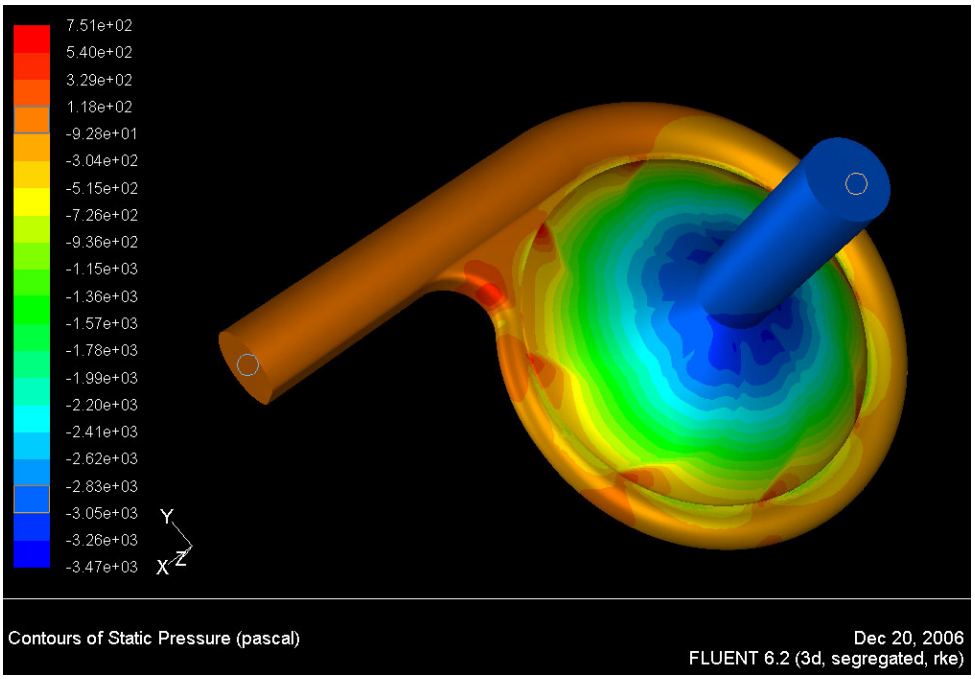

Figure 5.10: Pressure Distribution for Model 16 at Rotational Speed of 1000 rpm

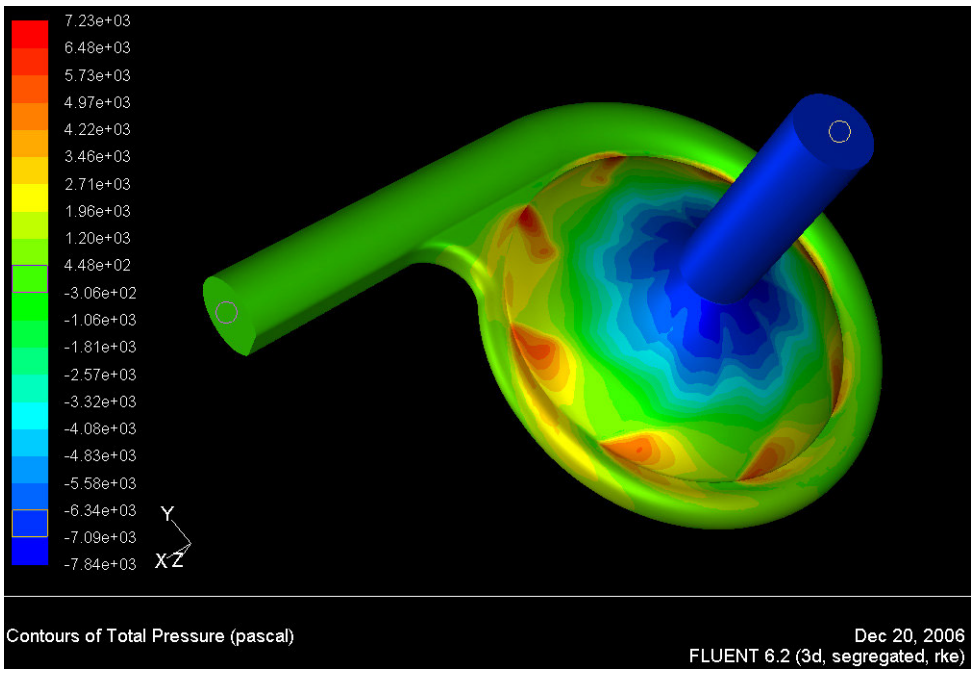

Figure 5.11: Pressure Distribution for Model 16 at Rotational Speed of 1500 rpm

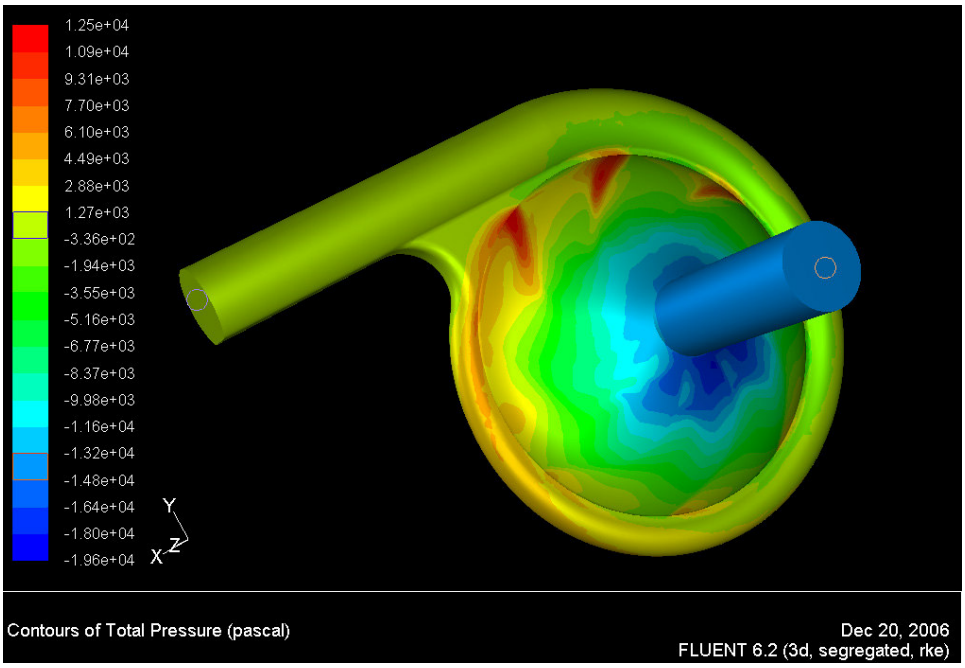

Figure 5.12: Pressure Distribution for Model 16 at Rotational Speed of 2000 rpm

5.3.2 Model 13

As a second produced design, the model 13 is chosen because from the CFD results it gives the best performance among the other designs. For this pump, only the profile of the impeller blade is changed, lower casing is modified for the new driving mechanism and the upper casing is kept untouched. The CAD models and products of the upper casing are shown in Figure 5.3 and 5.5. The CAD model of the Model 13 is shown in figure 5.13.

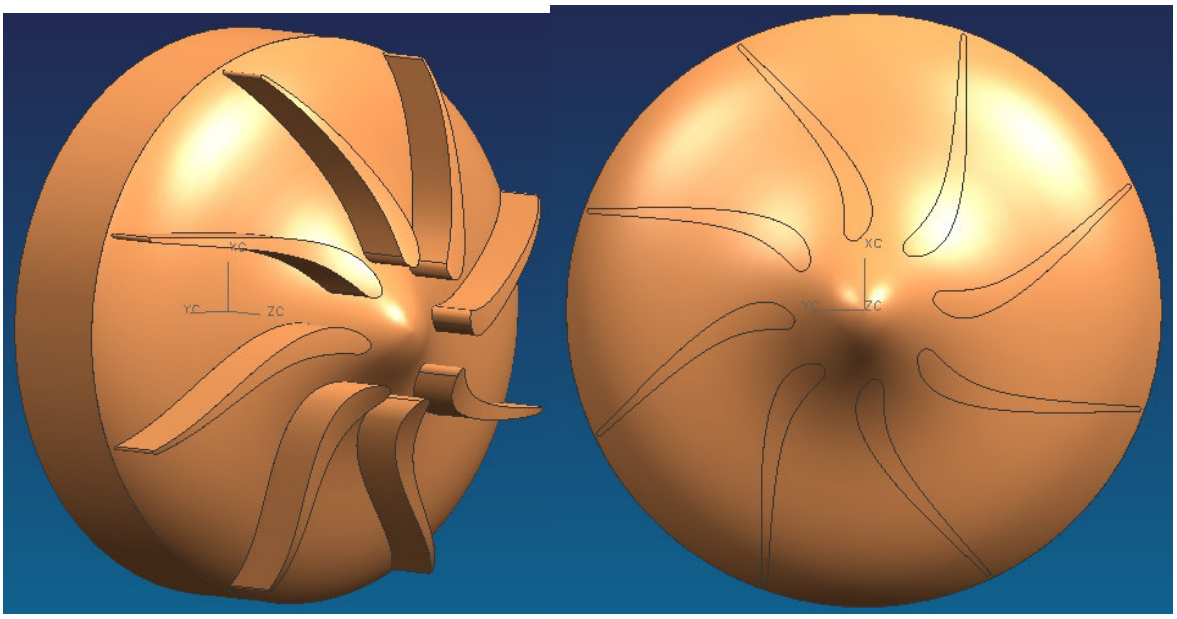

Figure 5.13: CAD model of the Impeller geometry of the model 13

On the other hand for this design a new driving mechanism is developed, so that the leakage from the bearing is eliminated. For this driving mechanism, there are Neodium magnets embedded under the body of the impeller. These 8 magnets are placed around the central axis of the shaft. The lower casing is modified according to the new longer shaft. On the motor side, there is a disk that carries also another 8 magnets those coincide with the magnets on the impeller. There is the lower casing between the disk and the impeller, so that there is no contact between these two rotating parts. Magnets are placed in a pole changing fashion that is North South North South etc in both disk and impeller. So the attraction force between these two parts is maximized. Figure 5.14 shows the CAD model of the impeller where the holes for the magnets are shown.

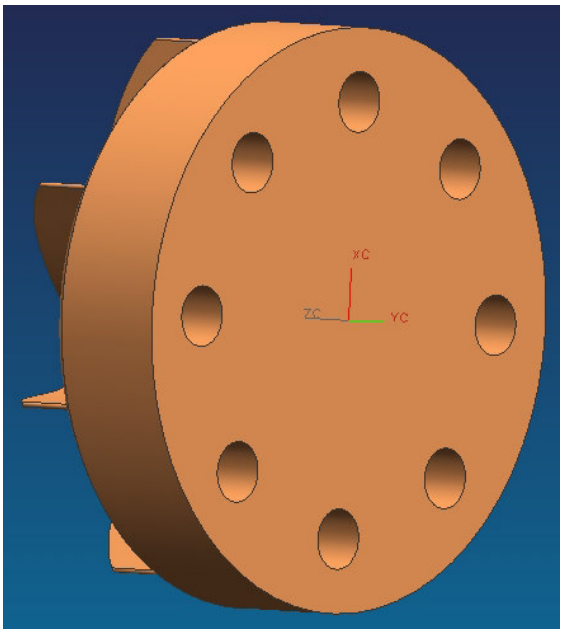

Figure 5.14: Holes of the magnets on the impeller's shaft

After following the CAD with CAM pump model 13 is produced. Figure 5.15 shows the produced impeller of this model.

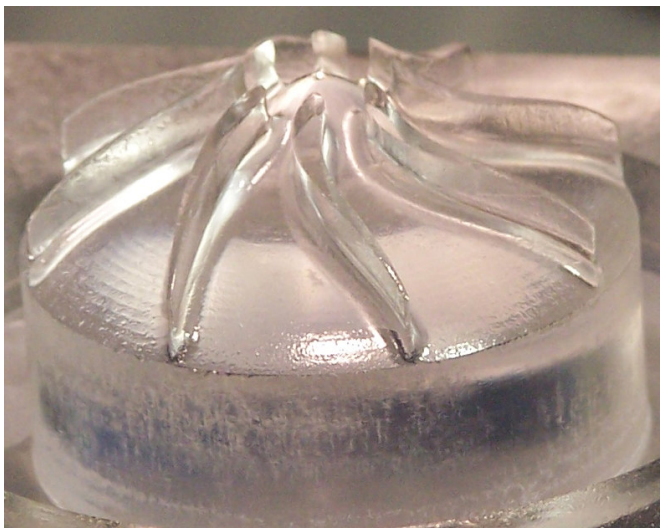

Figure 5.15: Produced Impeller of Model 13

On the other hand figure 5.16 shows the holes of the magnets on the impeller from the back side.

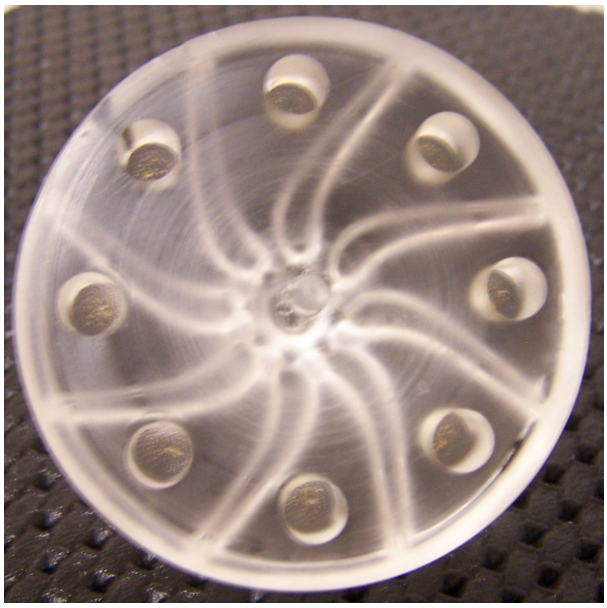

Figure 5.16: Holes of the magnets on the impeller model 13

The lower casing for this pump is shown in figure 5.17.

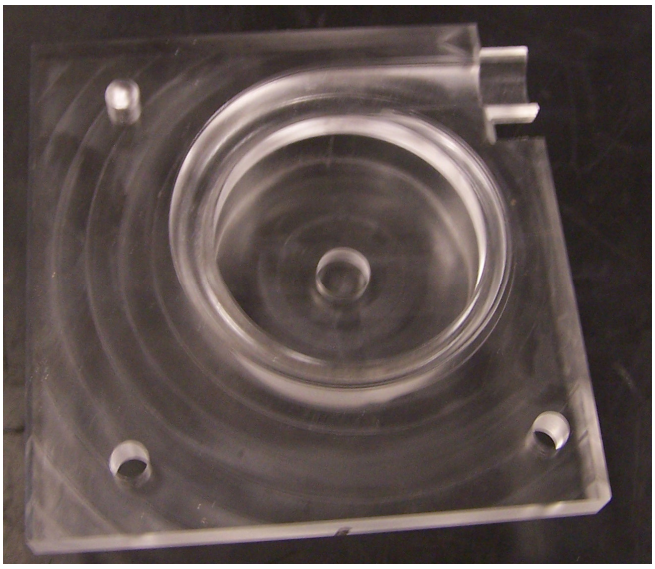

Figure 5.17: Lower casing for the pump of impeller model 13

The pump with the driving mechanism is shown in figure 5.18.

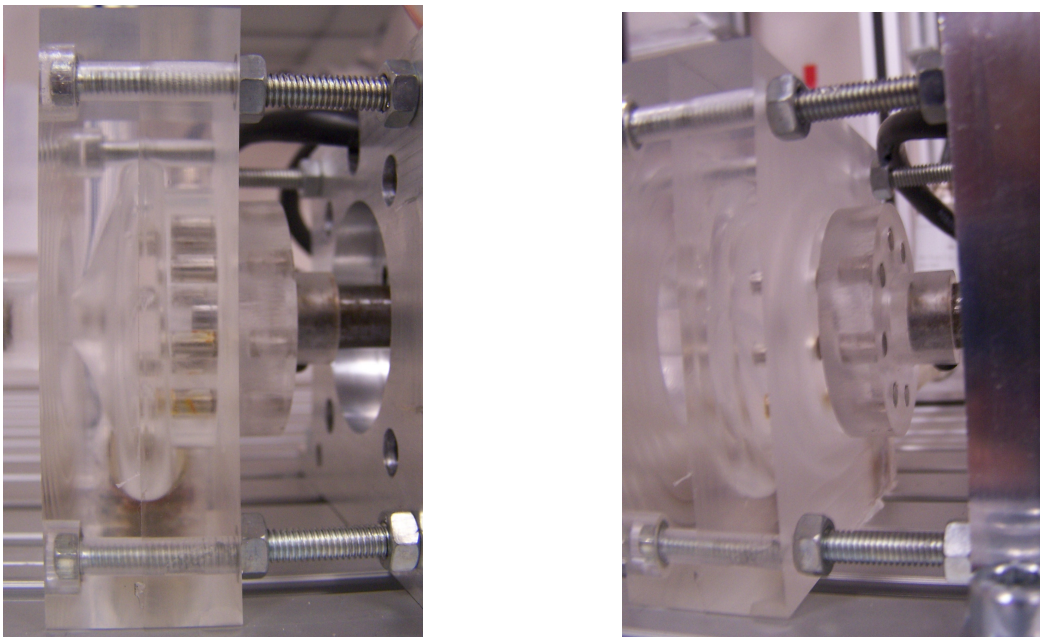

Figure 5.18: Driving Mechanism of Pump Model 13

Through this new designed driving mechanism there is no need for a hole on the lower casing for a shaft passing through it. Therefore the leakage problem from this hole is eliminated which was a big issue in the first design. There is no need to use any sealing mechanism. This lead to an increase in pumping performance and also it eliminated the misalignment problem of the axes of the impeller and the motor's shaft, because the misalignments on the order of 10 microns can be omitted with this driving system, which is another important problem with a through shaft driving mechanism.

For this new pump a new experimental setup is formed. In this setup there are two pressure sensors which give the inlet and the outlet pressures of the pump. There is also the flowmeter which gives the flow rate of the pump. These sensors are connected to a PC with a data acquisition card(DAQ) and the data is collected with the software named as CutPRO®. This new setup is shown in figure 5.19.

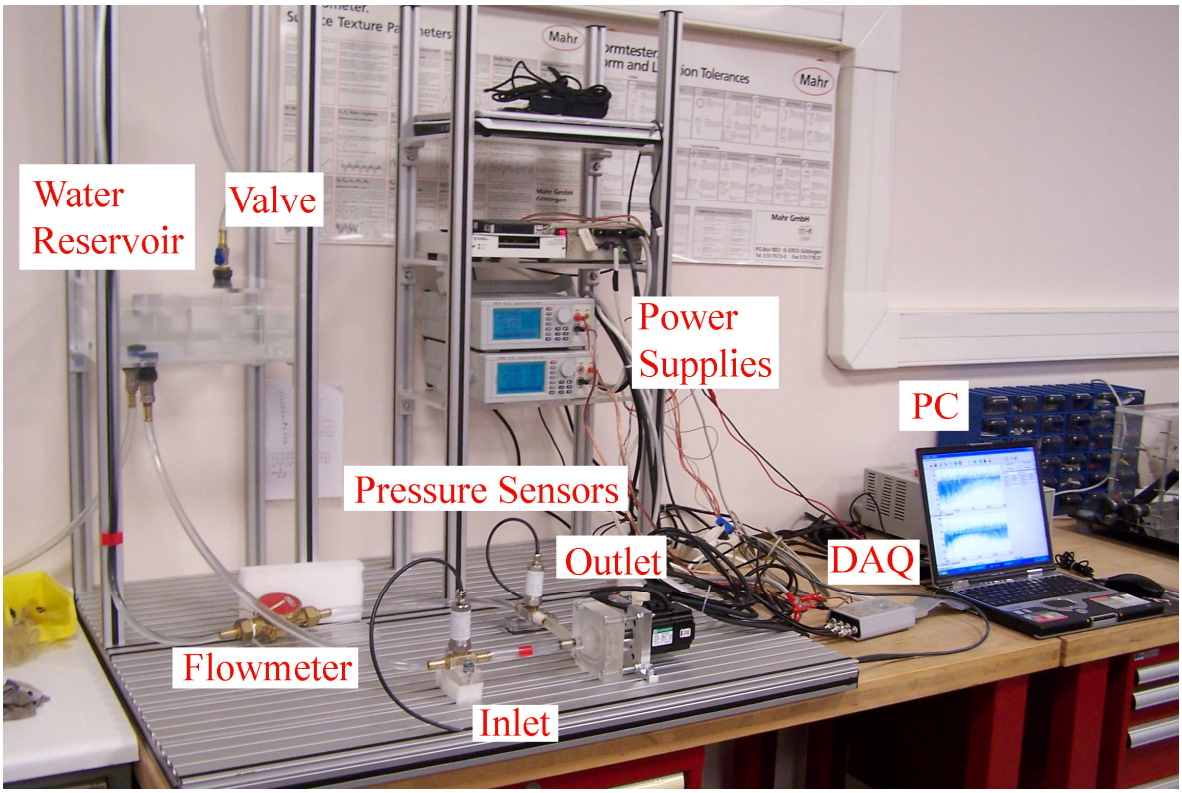

Figure 5.19: The Experimental Setup

For this pump, the experimental procedure is taken as follows:

The experiments are taken at 7 different rotational speeds. For each speed, by keeping the speed constant the flow rate is set at different values and the pressure difference is measured. By plotting these pressure differences with the flow rate data the characteristic behavior of the pump is observed. After the experimental measurements, the performance of the pump is examined by using CFD techniques. The results from CFD are compared with the experimental results.

The 7 different rotational speeds at which the experiments are carried are 1605rpm, 1805rpm, 1904rpm, 1953rpm, 2001rpm, 2257rpm and 2401rpm. The flow rate is limited by adjusting the valve. Then the pressure difference between the inlet and the outlet is measured. The results are shown in table 5.3 and plotted in figure 5.20.

Rotational Speed (rpm)	Flow Rate (L/min)	Flow Rate (kg/s)	Measured ΔP (mmHg)
1605	2,61	0,043	58,84
	2,31	0,038	62,24
	1,94	0,032	66,77
	1,13	0,019	72,41
	0,67	0,011	74,95
1805	2,86	0,048	74,13
	2,61	0,043	80,06
	1,76	0,029	88,19
	1,22	0,020	92,66
	0,85	0,014	94,55
1904	3,70	0,062	71,70
	3,25	0,054	76,90
	2,85	0,047	85,05
	2,33	0,039	95,64
	1,56	0,026	102,05
	1,16	0,019	104,71
	0,68	0,011	106,83
1953	3,86	0,064	74,48
	3,38	0,056	80,51
	2,67	0,045	93,13
	2,29	0,038	101,72
	1,54	0,026	108,18
	0,96	0,016	111,75

	0,60	0,010	113,25
2001	3,92	0,065	77,53
	3,31	0,055	87,91
	2,74	0,046	97,77
	2,35	0,039	106,84
	1,38	0,023	115,04
	1,12	0,019	116,51
	0,69	0,011	118,75
2257	4,44	0,074	90,42
	4,15	0,069	97,04
	3,74	0,062	108,65
	2,61	0,043	133,54
	1,75	0,029	141,50
	1,22	0,020	145,00
	0,99	0,016	146,50
	0,68	0,011	147,88
2401	4,72	0,079	101,48
	4,23	0,070	114,44
	3,65	0,061	131,21
	2,45	0,041	156,01
	1,57	0,026	163,20
	1,31	0,022	165,10
	0,94	0,016	167,19
	0,73	0,012	167,91

Table 5.3: Experimental Results for Model 13

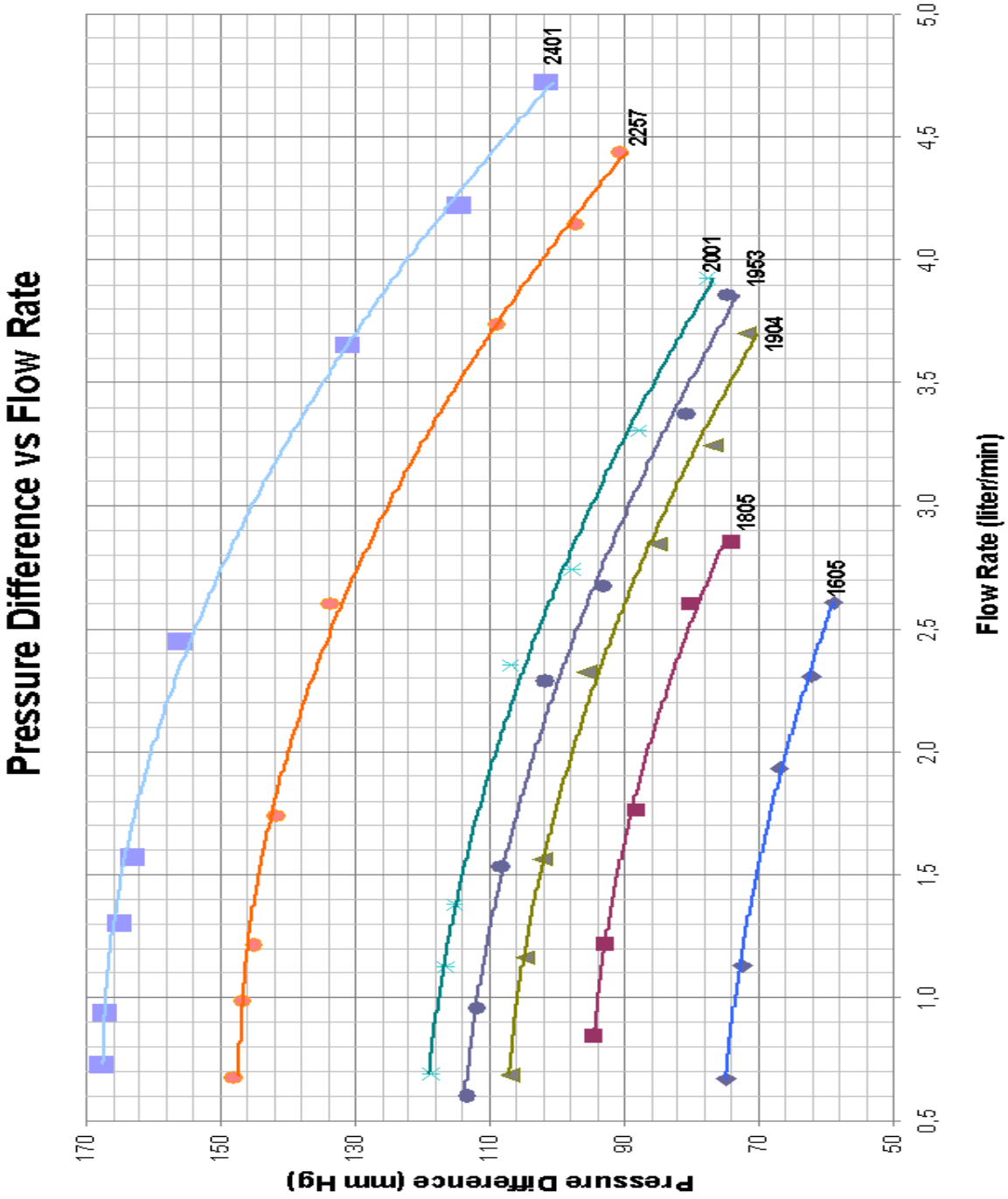

Figure 5.20: Experimental Results for Model 13

As it can be seen from the experimental results for a flow rate around 4.5 L/min a pressure difference of 100mmHg can be easily achieved for the rotational speed between 2257 and 2401 rpm. This criterion is determinant in the heart pump design. After the experimental procedure, in order to support the results of the computational method is carried out and for the rotational speeds 1953, 2001, 2257 and 2401 rpm the conditions are created in the computational environment. The CFD gives the pressure differences for each condition. Table 5.4 shows the computational results with the experimental results.

Rotational Speed (rpm)	**Flow Rate (L/min)**	**Calculated ΔP (mmHg)**	**Measured ΔP (mmHg)**	**% error**
1953	3,86	75,24	74,48	1,02
	3,38	86,48	80,51	7,42
	2,67	94,73	93,13	1,72
	2,29	102,61	101,72	0,88
	1,54	112,49	108,18	3,99
	0,96	113,11	111,75	1,22
	0,60	113,09	113,25	-0,14
2001	3,92	82,78	77,53	6,77
	3,31	97,32	87,91	10,71
	2,74	106,27	97,77	8,70
	2,35	113,5	106,84	6,24
	1,38	124,59	115,04	8,30
	1,12	125,55	116,51	7,76
	0,69	129,26	118,75	8,85
2257	4,44	101,51	90,42	12,26
	4,15	106,01	97,04	9,25

	3,74	115,21	108,65	6,04
	2,61	144,51	133,54	8,21
	1,75	152,56	141,50	7,82
	1,22	155,26	145,00	7,08
	0,99	157,12	146,50	7,25
	0,68	158,17	147,88	6,96
2401	4,72	108,37	101,48	6,80
	4,23	123,25	114,44	7,70
	3,65	137,95	131,21	5,14
	2,45	163,00	156,01	4,48
	1,57	164,40	163,20	0,74
	1,31	166,83	165,10	1,05
	0,94	171,41	167,19	2,53
	0,73	167,68	167,91	-0,13

Table 5.4: Computational Results vs. Experimental Results for Model 13

In order to see the relations between the computational and experimental results these are plotted. In figures 5.21, 5.22, 5.23, and 5.24 the agreement between the computational results and experimental results can be seen. From the percentage error, for low speeds and low flow rates the error in the prediction small. However if the rotational speed and the flow rate increases the errors in the predictions increase. This is because of the turbulences in the flow. Turbulence affects the error made in computational methods.

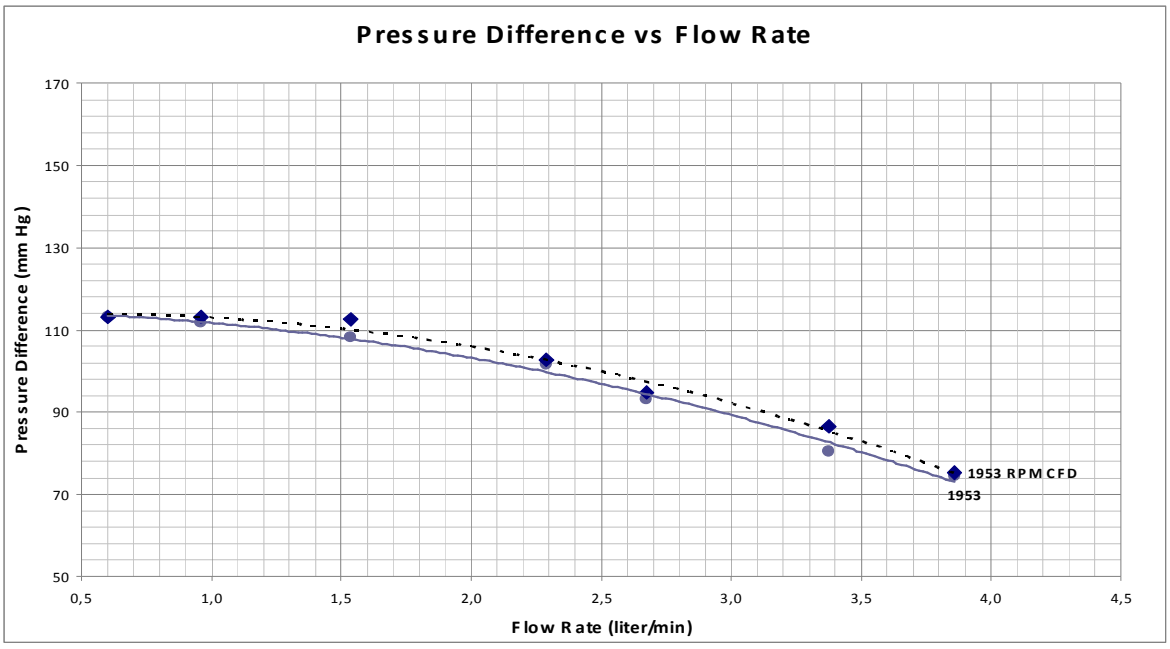

Figure 5.21 : CFD Results vs. Experimental Results for 1953 RPM

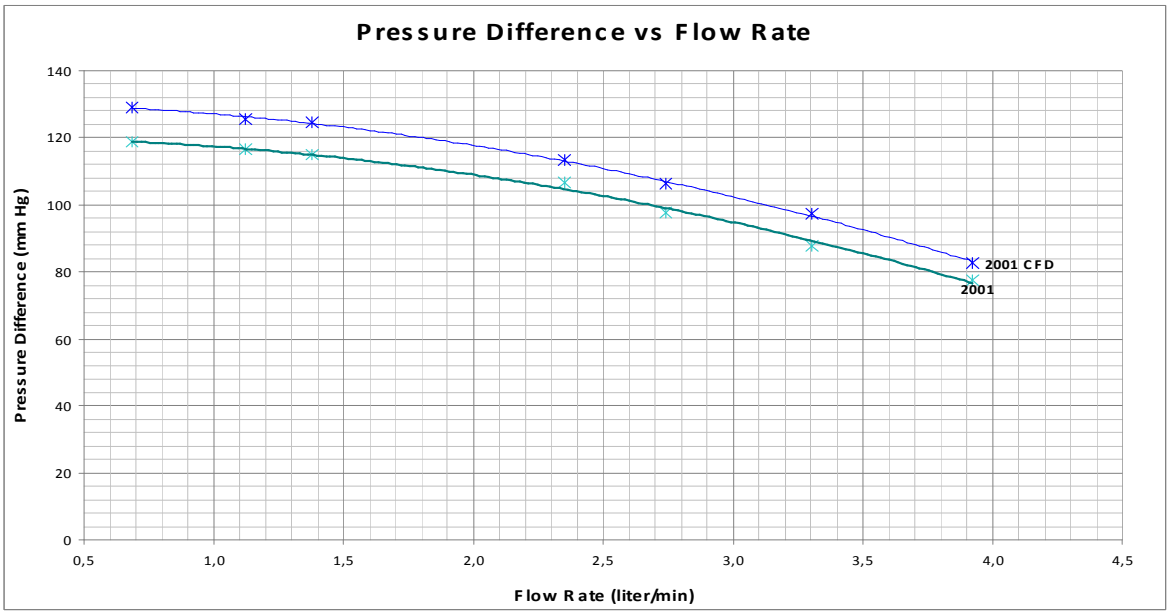

Figure 5.22 : CFD Results vs. Experimental Results for 2001 RPM

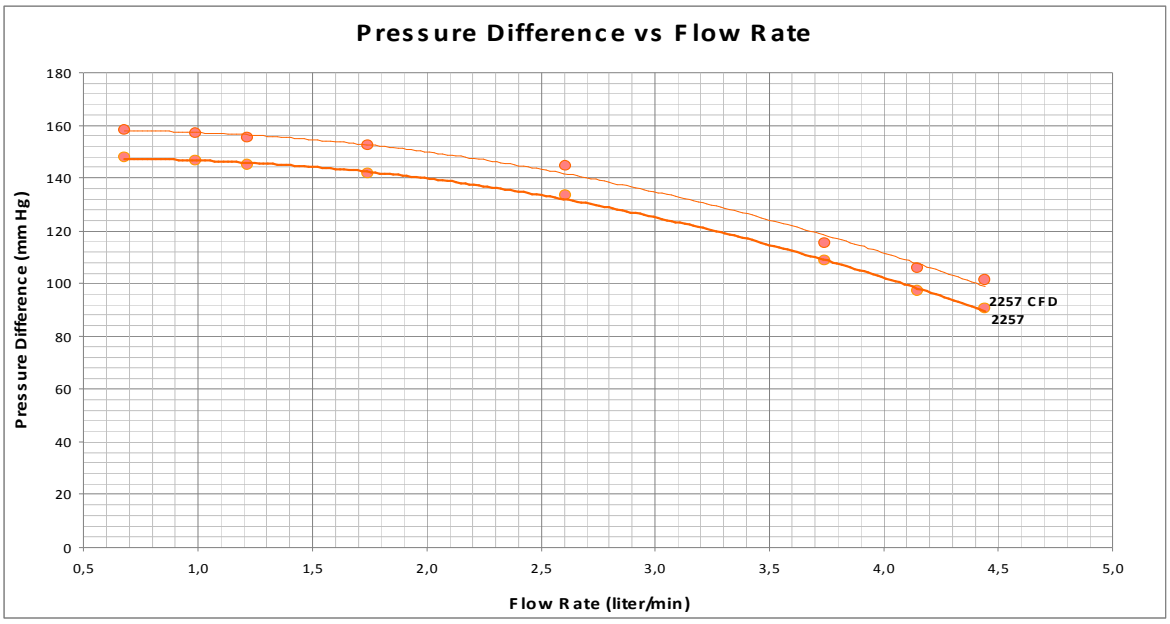

Figure 5.23 : CFD Results vs. Experimental Results for 2257 RPM

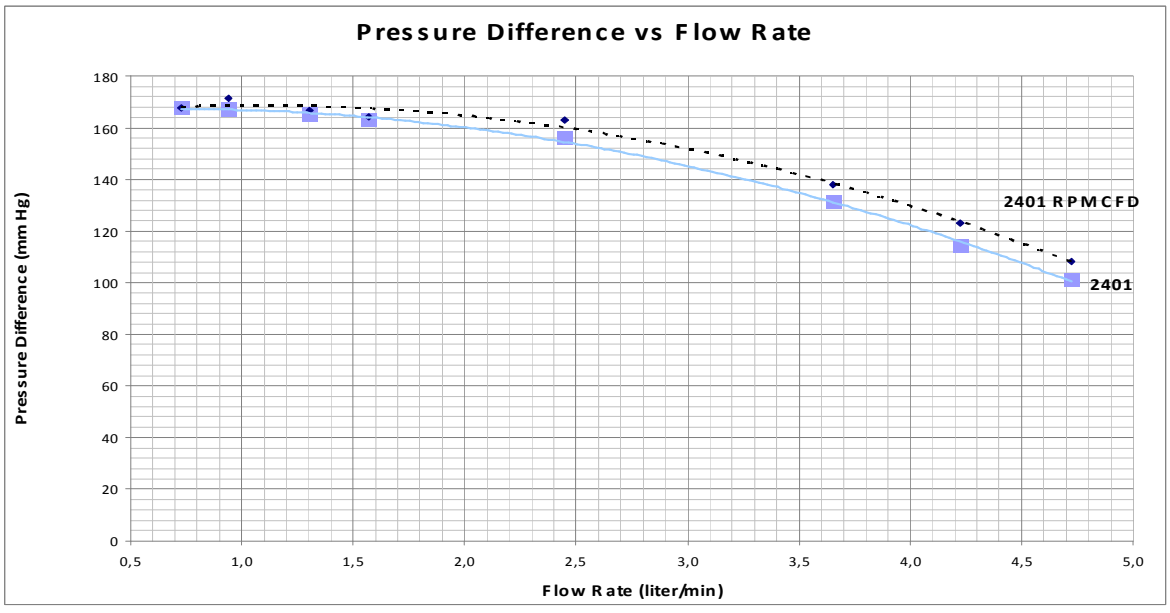

Figure 5.24 : CFD Results vs. Experimental Results for 2401 RPM

As it can be seen from the figures 5.21, 5.22, 5.23 and 5.24 the theoretical and experimental results are in good agreement. The performance curves of the pump suggest that this pump design can be used as a Left Ventricular Assist Device.

5.4 Comparison of Airfoil Shaped and Conventional Blades

Another aim of this research was to find out if the airfoil shaped blades are more advantageous or disadvantageous than the conventional blades. For this approach an impeller of the conventional blades is produced with the same flow volume of the impeller model 13. The blades' heights are 5 mm for both impellers, and the diameters are 48.3 mm for both impellers. The CAD model of the impeller of the conventional blades is shown in figure 5.25.

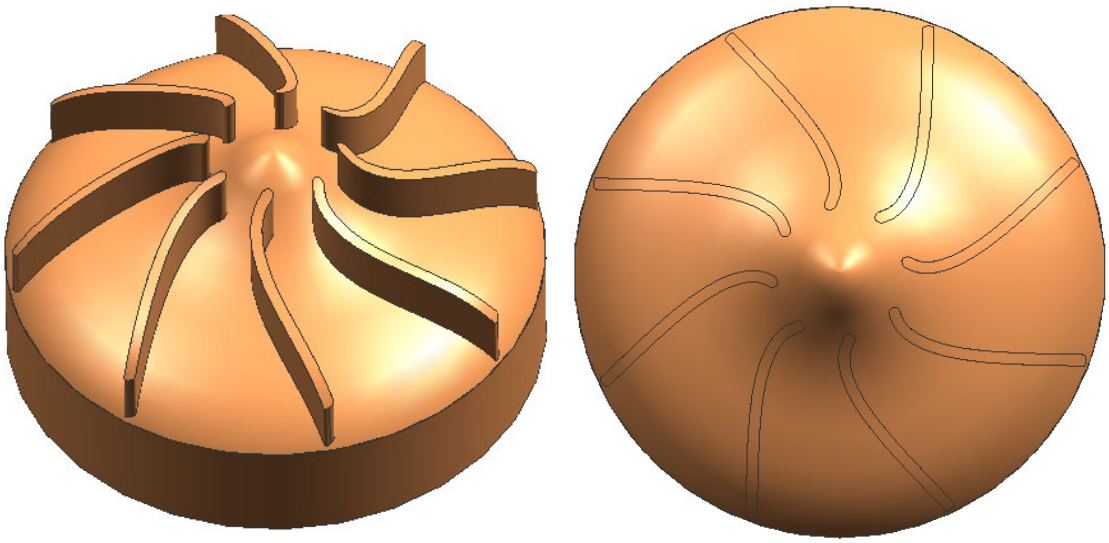

Figure 5.25: CAD Model of the Impeller of with constant blade thickness

This model is produced with the CNC machine in MARC. The produced impeller is shown in figure 5.26.

Figure 5.26: Produced Impeller of constant blade thickness

In figure 5.27, the constant blade thickness impeller and the impeller of blades shaped as airfoil is shown together.

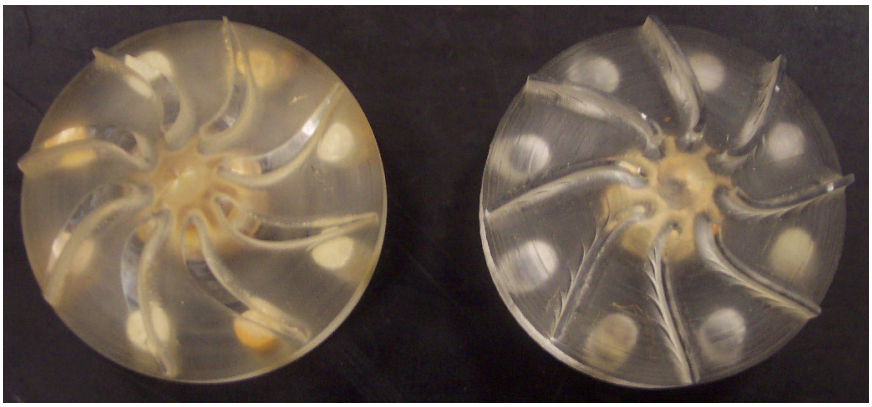

Figure 5.27: Airfoil Shaped and Constant Thickness Blade Impellers

The tests are run for both impellers and the results are presented in figure 5.28. As the figure 5.28 suggests the impeller with blades of airfoil geometry performs better than the

impeller of the conventional blades at most all of the points for the speeds 2250 rpm and 2000 rpm.

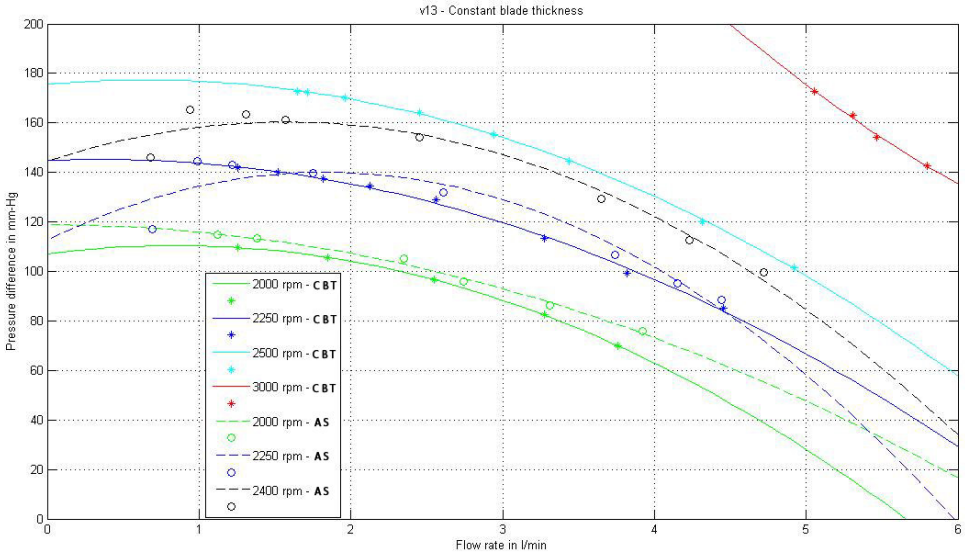

Figure 5.28: Test Results for Airfoil Shaped and Constant Blade Thickness Models

Chapter 6

CONCLUSION & FUTURE WORK

The objective of the thesis has been to develop a reliable and permanently implantable centrifugal blood pump as a left ventricular assist device. Special emphasis was placed on the geometric factors of an impeller and their effects on the performance of the pump and secondly several designs were examined and two of them are produced and their performances are tested. In prediction of the performance of the centrifugal pumps, the computational fluid dynamics (CFD) was used. The Fluent®, the commercial package for CFD was used. The results of this study provide the method for designing the centrifugal blood pumps for specific performance criteria, the predicting the performance of the pump and the producing and testing of the pump.

The base of the design of the pump was the design of the impeller geometry. The blade geometry affects the performance most significantly. Therefore the geometric parameters of the blades were the main focus of this study. To define a blade there should be eleven parameters defined. Four of them chosen as to be variable and observed their effects on the performance. For each different value of a variable a unique blade and impeller is designed. These different designs were examined first by using CFD techniques.

The CFD results showed the significant effects of the blade geometry and two of them were chosen to be produced. These were most efficient geometries. The Computer Numerically Controlled (CNC) Machine in Manufacturing and Automation Research Center (MARC) was used for the production process. First the geometries were designed by using a Computer Aided Design (CAD) tool, which was Unigraphics®. In

Unigraphics® the tool paths and G-codes were developed to control the CNC machines. According to the simulations of the tool paths the impellers and the covers of the pump is produced.

While developing the most efficient impeller geometry different driving mechanisms for the impeller were developed. First driving mechanism was the direct driving mechanism with a shaft under the impeller, which was connected to the motor's shaft with a mechanic coupling. In this system the impeller's shaft is connected to motor's shaft through a hole on the cover of the pump, which yielded to losses in pump's performance. This system was developed to a magnetically coupled driving mechanism. In this system, there is no need for a shaft under the impeller; rather there were Neodium magnets placed as a circular array. On the motor side, there was an apparatus which carried the same circular array of the magnets to form the attraction forces. Through these attraction forces there is no need for a hole on the cover. Both of these mechanisms were applied and tested.

To test the produced pumps, an experimental setup is developed. In this setup there is a water reservoir to supply the pump. There are two pressure sensors to measure the pressures on the inlet and outlet of the pump. There is also a flowmeter to measure the flow rate. There is a valve to arrange the flow rate. There is a PC and DAQ card to collect the measured data and perform the analysis.

According to the test results the model 13 meets the hydrodynamic needing of a human heart suffering from diseases. On the other hand, the effects of the pump to the blood cells should be examined as a future work. The blood should be used as the test fluid and the system should be run for one to four months. After the operations the blood should be examined if the hemolysis and/or thrombus formed or not. If the index of hemolysis is under the risky limit, the pump can be thought to be capable for good hemodynamic support for the patients. After this stage the pump should be tested with animals, and according to these results it should be considered to be applicable or not to the humans.

BIBLIOGRAPHY

[1] Y. Nose, Design and Development Strategy for the Rotary Blood Pump, Artificial Organs, 22(6):438 -446 (1998)

[2] J.W. Cameron, Centrifugal Pumps, London : Merchant Books, (2006)

[3] H. Moustapha, M. F. Zelesky, N. C. Baines, D. Japikse, Axial and Radial Turbines, White River Junction, Vt. : Concepts NREC, (2003)

[4] D. G. Shepherd, Principles of Turbomachinery, The Macmillan Company, (1971).

[5] X.Song, H. G. Wood, S. W. Day, and D. B. Olsen, Studies of Turbulence Models in a Computational Fluid Dynamics Model of a Blood Pump, Artificial Organs, 27(10):935-937 (2003)

[6] L. Xian-hua, Z. Shu-jia, Z. Bao-lin, H. Qing-bo, The Study of the k – ε Turbulence model for Numerical Simulation of Centrifugal Pump (2006)

[7] T.H. Shih, W.W.Liou, A. Shabbir, Z. Yang and J. Zhu, A New k – ε Eddy Viscosity Model for High Reynolds Number Turbulent Flows, Comput Fluids 24, pp.227-238, (1995)

[8] D.C. Wilcox, Turbulence Modeling for CFD, La Cãnada,Calif: DCW Industries, (1998)

[9] S. Wesolowski, The Role of the Pulse in Maintenance of the Systemic Circulation During Heart – Lung Bypass, Artificial Organs, 1:84 – 6 (1956)

[10] G. Saxton, C. Andrews, An Ideal Pump with Hydrodynamic Characteristics Analogous to the Mammalian Heart, Artificial Organs, 6:288 – 9 (1960)

[11] E. Rafferty, H. Kletschka, M. Wynyard, J. Lackin, L. Smith, B. Cheathem, Artificial Heart II – Application of Nonpulsatile Radially Increasing Pressure Gradient Pumping Principle, Minn Med 52:191 (1968)

[12] F. Dorman, E. Bernstein, P. Blackshear, R. Sovilj, D. Scott, Progress in the Design of a Centrifugal Cardiac Assist Pump with Transcutaneous Energy Transmission by Magnetic Coupling, Artificial Organs 15:441 – 8 (1969)

[13] E. Bernstein, L. Consentino, S. Reich, P. Stasz, I. Levine, D. Scott, F. Dorman, P. Blackshear, A Compact, Low Hemolysis, Nonthrombogenic System for Nonthoracotomy prolonged Left Ventricular Bypass, Artificial Organs 20:643 – 54 (1974)

[14] L. Golding, F. Loop, M. Peter, G. Jacobs, C. Gill, L. Groves, Y. Nose, Use of a Temporary Left Ventricular Assist System Postoperatively, Artificial Organs 3:394 (1979)

[15] L. Golding, G. Jacobs, T. Murakami, S. Takatani, F. Valdes, H. Harasaki, Y. Nose, Chronic Nonpulsatile Blood Flow in an Alive, Awake Animal 34-day Survival, Artificial Organs, 26:251-5 (1980)

[16] G. Bramm, P. Novak, D. Olsen, Blood Pump for Long Term Application with a Noncontacting, Magnetically Suspended Rotor to Reduce Blood Trauma, Artificial Organs 11:26-9 (1981)

[17] G. Bramm, P. Novak, D. Olsen, A Free Floating Body as a Rotor of a Centrifugal Pump for LVAD or TAH, Artificial Organs, 8:441-5 (1981)

[18] G. Bramm, D. Olsen, Blood Pump with a Magnetically Suspended Impeller, Artificial Organs, 31:79-83 (1985)

[19] R. Wampler, J. Moise, O. Frazier, D. Olsen, In Vivo Evaluation of a Peripheral Vascular Access Axial Flow Blood Pump, Artificial Organs 34:450 (1988)

[20] J. Monties, T. Mesana, P. Havlik, J. Trinkl, J. Demunck, B. Candelon, Another Way of Pumping Blood with a Rotary but Non-centrifugal Pump for an Artificial Heart, ASAIO Trans, 36(3):258-60 (1990)

[21] T. Takeuchi, K. Nishimura, H. Okabayashi, Y. Okamoto, T. Ban, T. Akamatsu, T. Shiroyama, H. Hokimoto, T. Fujita, Y. Shibata, Experimental Study of Mutating Centrifugal Blood Pump in Vivo, Artificial Heart & Heart Replacement, 93-9 (1990)

[22] I. Sakuma, S. Takatani, Y. Nose, Development of a Motor Driven Sealless Centrifugal Blood Pump, Proceedings International Workshop Rotary Blood Pumps 48-53 (1991)

[23] T. Fossum, D. Morley, R. Benkowski, E. Tayama, D. Olsen, G. Burns, M. Miller, J. Franks, E. Martinez, G. Carroll, J. Edwards, A. Vinnerqvist, B. Lynch, F. Stein, G. Noon, M. DeBakey, Chronic Survival of Calves Implanted with the DeBakey Ventricular Assist Device, Artificial Organs, 23(8):802-6 (1999)

[24] K. Butler, T. Maher, H. Borovetz, R. Kormos, J. Antaki, M. Kameneva, B. Griffith, T. Zerbe, F. Schaffer, Development of an Axial Flow Blood Pump LVAS, ASAIO Journal, 38:M296-300 (1992)

[25] M. Macris, T. Myers, R. Jarvik, In vivo Evaluation of an Intraventricular Electric Axial Flow Pump for Left Ventricular Assistance, ASAIO Journal, 40:M719-22 (1994)

[26] R. Ottenberg, C. L. Fox, The Rate of Removal of Hemoglobin from the Circulation and its Renal Threshold in Human Beings, Am J Physiol 123: 516-525, (1938)

[27] N.S.R. Maluf, Effect of Electrical Stimulation of Medial Popliteal Nerve On Caliber of Renal Arteries in Unanesthetized Man, Angiology 5: 537-553 (1949)

[28] M. Girard, H. Latham, S. Penman, J.E. Darnell Entrance of newly formed Messenger RNA and Ribosomes into Hela Cell Cytoplasm J Mol Biol. 11:187–201 (1965)

[29] Prof. Dr. Süha Küçükaksu , "Türkiye'den 'yapay kalp pompası' atağı", Anadolu Ajansı, (2006)

VITA

Gökhan Yıldız completed the high school in Üsküdar Fen Lisesi, İstanbul, in 2000. He received his B.Sc. Degree in Mechanical and Electrical-Electronics Engineering from Koç University (KU), İstanbul, in 2005. Since 2005, he is in the M.Sc program in Mechanical Engineering at Koc University as a teaching/research assistant. As his graduation project he has been developed a Laser Doppler Vibrometry a departmental project in KU, Istanbul, Turkey designing and manufacturing a Laser Doppler Vibrometry based on self-mixing effect. For the completion of the program he has taken part in a mechanical engineering thesis study with the title 'From Concept to the Prototype of Heart Turcica Centrifugal: Development of the First Implantable Centrifugal Left Ventricular Assist System in Turkey'.